

A chronological and chemical zircon study of some pegmatite dikes and lenses from the central part (Ayoquezco-Ejutla) of the Oaxacan Complex, southern Mexico

Valentina Shchepetilnikova^{1,*}, Jesús Solé², Luigi Solari³, and Fanis Abdullin¹

¹ Posgrado en Ciencias de la Tierra, Instituto de Geología, Universidad Nacional Autónoma de México, Ciudad Universitaria, 04510 Coyoacán, México D.F., Mexico.

² Instituto de Geología, Universidad Nacional Autónoma de México, Ciudad Universitaria, 04510 Coyoacán, México D.F., Mexico.

³ Centro de Geociencias, Universidad Nacional Autónoma de México, Campus UNAM Juriquilla, Blvd. Juriquilla No. 3001, Querétaro, 76230, Mexico.

* *shchepetilnikova@gmail.com*

ABSTRACT

We carried out a geochronological and geochemical study of zircons from seven pegmatite intrusions collected from the central part (Zimatlán-Ayoquezco-Ejutla villages) of the Oaxacan Complex, southern Mexico. U-Pb ages and trace element chemistry were obtained by laser ablation inductively coupled plasma mass spectrometry (LA-ICP-MS). The objective of this work is to determine the time of pegmatite emplacement and its high grade metamorphism, if present, by U-Pb dating and identify its possible source and crystallization environment, using trace element concentrations in zircons. The geochronological study allowed to distinguish three main groups of pegmatites: post-tectonic, syntectonic, and pre-tectonic with respect to the granulite facies metamorphism event, which have ages in the ranges of 963 ± 7 to 977 ± 5 Ma, 980 ± 5 to 981 ± 7 Ma, and 1190 ± 7 to 1201 ± 5 Ma, respectively. The REE geochemistry in pegmatite zircons shows that the mechanism of pegmatite formation was in some cases magmatic, in others metamorphic or in between. It has been suggested before that all pegmatites of this region are "granitic" and are the result of a classical evolution of a felsic melt formed *in situ* during the anatexis of the Oaxacan Complex rocks. The interpretation of our chemical data indicates that the composition of the initial melt, from which each class of pegmatite was formed, can be ultramafic, alkaline or carbonatitic, and only one sample shows a granitic-like initial composition. This means that the pegmatites of the Oaxacan Complex are of diverse origin and only those of quartz-feldspar mineralogy are actually granitic in origin.

Key words: Oaxacan Complex; pegmatite; zircon; rare earth elements; U-Pb geochronology.

RESUMEN

Hemos realizado un estudio geocronológico y geoquímico de los circones de siete pegmatitas colectadas en la zona central (Zimatlán-Ayoquezco-Ejutla) del Complejo Oaxaqueño, Sur de México. Las

*edades U-Pb y los elementos traza se obtuvieron mediante LA-ICP-MS. El objetivo de este trabajo es determinar la edad de emplazamiento de cada pegmatita y su metamorfismo de alto grado, si está presente, mediante datación U-Pb, así como identificar su posible roca fuente y ambiente de cristalización, usando los elementos traza en circón. Este estudio geocronológico ha permitido identificar tres grupos de pegmatitas: sintectónicas, post-tectónicas y pre-tectónicas, con respecto del evento metamórfico granulítico, que presentan edades en los rangos de 963 ± 7 a 977 ± 5 Ma, 980 ± 5 a 981 ± 7 Ma, y 1190 ± 7 a 1201 ± 5 Ma, respectivamente. La geoquímica de REE en circones muestra que el mecanismo de formación de las pegmatitas en algunos casos fue magmático, en otros – metamórfico, o una combinación de los dos. Se ha sugerido previamente que todas las pegmatitas de esta región son "graníticas" y son el resultado de la evolución clásica de un magma félsico formado *in situ* durante los procesos de anatexis de las rocas del Complejo Oaxaqueño. La interpretación de los análisis químicos indica que la composición inicial del fundido del cual derivan los cuerpos pegmatíticos puede ser ultramáfico, alcalino o carbonatítico, y sólo una muestra presenta una composición granítica original. Esto significa que las pegmatitas del Complejo Oaxaqueño son de origen diverso y sólo las de mineralogía cuarzo-feldespática son de origen granítico.*

Palabras clave: Complejo Oaxaqueño; pegmatita; circón; elementos de las tierras raras; geocronología U-Pb.

INTRODUCTION

The Oaxacan Complex constitutes the largest (10000 km²) outcrop of ~1 Ga rocks in Mexico. From the regional point of view, the Oaxacan Complex is the largest exposure of the NW-SE extending Oaxaquia microcontinent (e.g., Ortega-Gutiérrez *et al.*, 1995), underlying most of the Mexican territory. Oaxaquia is a portion of the Grenville-aged belt in the North American continent, extending from northeastern Canada to Southern Mexico (Ruiz *et al.*, 1999) (Figure 1a).

Till now, the pegmatites of the Oaxacan Complex have not received much attention, in spite of their importance for the understanding of

the Mexican Grenville basement. Pegmatite formation processes in this region are closely related to the tectonic history of the Oaxacan Complex (e.g., Solari *et al.*, 2003; Prol-Ledesma *et al.*, 2012). The first published ages of the Oaxacan Complex rocks were obtained from pegmatite zircons with the Pb- α method, yielding ages in the range of 960 – 1110 Ma (Fries *et al.*, 1962; Fries and Rincón-Orta, 1965).

Most of the pegmatites in the world contain zircon in trace quantities only, but its abundance increases as pegmatite compositions become more alkaline (London and Černý, 2008). Some well-known pegmatites of the Oaxacan Complex contain abundant zircon megacrysts (e.g., Fries *et al.*, 1962; Fries and Rincón-Orta, 1965; Haghenbeck-Correa, 1993; Arenas-Hernández, 1999; Prol-Ledesma *et al.*, 2012).

Zircon is considered to be one of the first phases to crystallize in most igneous rocks (Nagasawa, 1970) and is enriched in REE, Y, Th, U and Hf. The concentrations of these elements in zircons may provide information concerning the nature of the primary melt (e.g., Nagasawa, 1970; Pupin, 2000; Belousova *et al.*, 2002; Hoskin and Schaltegger, 2003; Lesnov, 2012). Moreover, the morphology of zircon crystals can give information about formation conditions (Pupin, 1980). Due to its chemical resistance and ability to survive weathering and transport processes, as well as high temperature metamorphism and anatexis, zircon is able to record information about conditions and time of its crystallization and recrystallization (Belousova *et al.*, 2002).

In this paper we present new zircon U-Pb ages obtained by laser ablation inductively-coupled plasma mass spectrometry (LA-ICP-MS)

and provide trace element chemistry of seven zircon samples collected from pegmatites located in the central part of the Oaxacan Complex, between the villages of Zimatlán, Ayoquezcó, and Ejutla (Figures 1b and 1c). The objective of this work is to determine the time of pegmatite emplacement and its high-grade metamorphism, as well as to identify the possible source rock types and crystallization environment.

GEOLOGICAL FRAMEWORK

The Oaxacan Complex consists of a diversity of rock types that were metamorphosed up to the granulite facies and were derived from either a sedimentary protholith (marbles, calcsilicates, quartzo-feldspathic and graphitic gneiss) or from igneous rocks (granite, tonalite, syenite, gabbro, anorthosite, charnockite). Other igneous rocks are present in the form of pegmatite intrusions (Fries *et al.*, 1974; Bloomfield and Ortega-Gutiérrez, 1975; Ortega-Gutiérrez *et al.*, 1977; Keppie *et al.*, 2003). According to Solari *et al.* (2003), these rocks were involved in two tectonothermal events during the Grenville orogeny: the Olmecan event (1106 ± 6 Ma), and the Zapotecan event (1004 ± 3 to 979 ± 3 Ma). The existence of the former event was recently questioned by Weber *et al.* (2010), who did not find its evidence in the southernmost edge of the Oaxacan Complex, near Pluma Hidalgo (Oaxaca). The temperature and pressure conditions of the Zapotecan granulite facies event were $700 - 825$ °C at $7.2 - 8.2$ kb (Mora *et al.*, 1986) in the northern part and

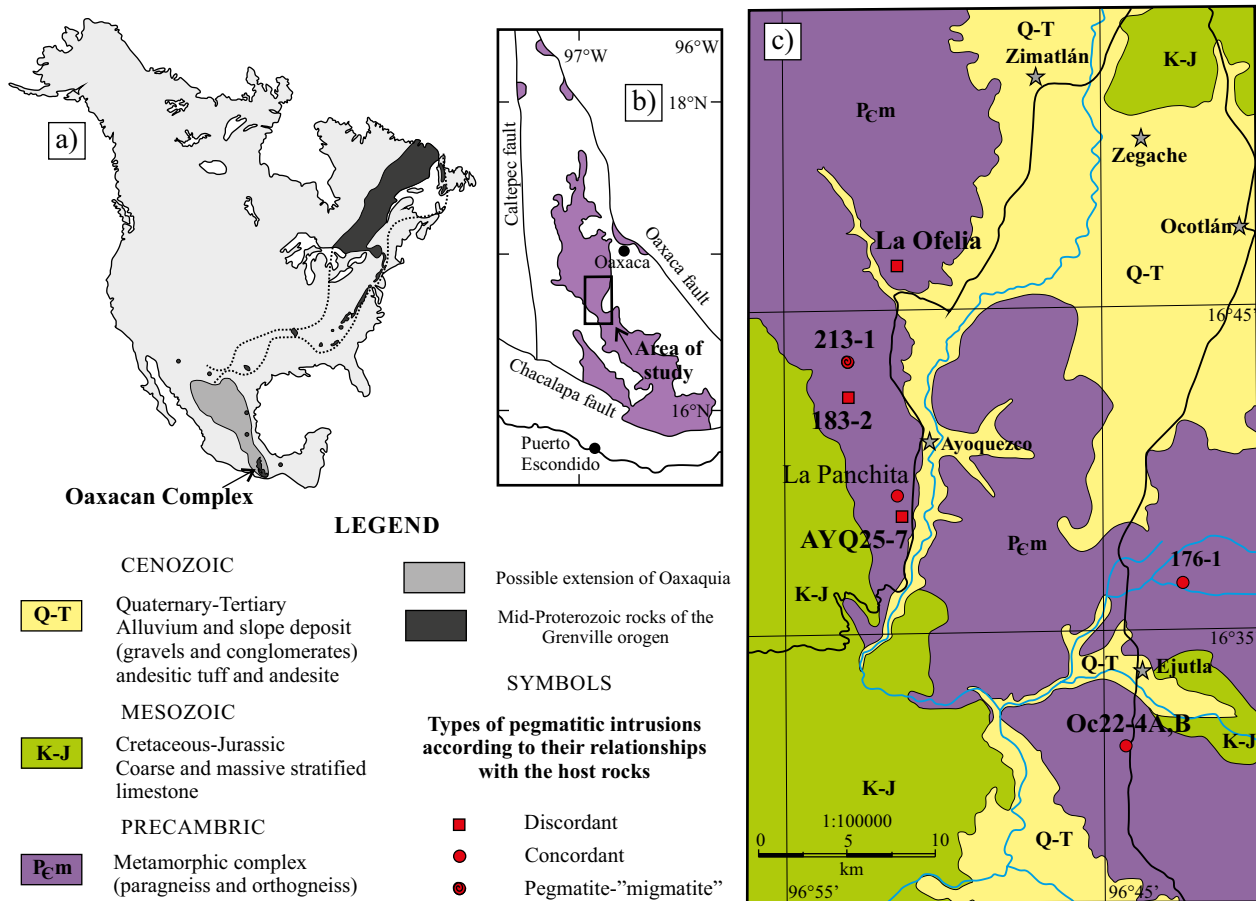


Figure 1. a) and b) Location of the Oaxacan Complex, Oaxaquia and other outcrops of Mid-Proterozoic rocks of the Grenville orogeny in North America; dotted lines – possible extension of the Grenville age rocks (redrawn from Gillis *et al.*, 2005). c) Simplified geological map from the studied Zimatlán-Ayoquezcó-Ejutla area, modified from Elias-Herrera and Obregón-Ramos (1983), with sample locations indicated.

800 – 900 °C at 8 kb in the southern portion of the Oaxacan Complex (Schulze-Schreiber, 2011).

There is a large age gap between the end of the Grenville orogeny and the deposition of the oldest discordant unit above the Oaxacan Complex, the Early Ordovician sedimentary marine rocks from Tiñú Formation (Pantoja-Alor and Robinson, 1967). This formation is only found in the northern Oaxacan Complex, whereas in the southern part the stratigraphic constraints are <500 m thick Jurassic red beds (?) and Cretaceous platform carbonate rocks and flysch (Schulze-Schreiber *et al.*, 2004).

The Oaxacan Complex contains multiple pegmatite dikes that are either concordant or discordant, with respect to the host rock foliation. Some of these pegmatites are undeformed and others show features of syntectonic deformation (Schaaf and Schulze-Schreiber, 1998; Solari *et al.*, 1998). In the northern Oaxacan Complex, Solari *et al.* (2003) reported the presence of at least three types of pegmatites, which, based on their relationships with the Grenvillian deformation, were classified as pre-tectonic, syntectonic, and post-tectonic. The central part of the Oaxacan Complex, south of Oaxaca City, between Zimatlán, Ejutla, and Ayoquezco, is also characterized by multiple pegmatitic intrusions, but to this day there is only little information published on this topic (Elías-Herrera and Obregón-Ramos, 1983). In general, all the pegmatites belonging to this sector and mentioned in literature, are dikes or lenses with very coarse-grained textures and were identified as late-tectonic granitic pegmatites, formed by partial melting of the host rock gneisses (Haghenbeck-Correa, 1993; Arenas-Hernández, 1999). Only few of these pegmatites were previously dated by K-Ar, Rb-Sr or Pb- α , with ages in the range of 670 – 980 Ma (Fries and Rincón-Orta, 1965; Fries *et al.*, 1962; Anderson and Silver, 1971; Ortega-Gutiérrez *et al.*, 1977).

For this study seven pegmatites in the central part of the Oaxacan Complex were chosen. Three of them have already been mentioned in literature (La Ofelia, La Panchita, and OC22-4AB) (*e.g.*, Fries and Rincón-Orta, 1965; Anderson and Silver, 1971; Arenas-Hernández, 1999). The remaining four were discovered during the field work (183-2, 176-1, 213-1 and AYQ25-7). All pegmatites and pegmatites-migmatites (leucosome) are characterized by the presence of zircon and, in some cases, show a very unusual mineralogy for a “granitic” pegmatite (London and Černý, 2008). Among the most remarkable minerals, they contain scapolite, clinopyroxene and primary calcite.

La Ofelia, 213-1, 183-2, La Panchita, and AYQ25-7 are located in the western part, OC22-04 and 176-1 are located in the eastern part of the study area. The pegmatite bodies OC22-04 and 213-1 have lenticular forms following the foliation of the host rocks (Figure 1c). The La Ofelia, 176-1, La Panchita, 183-2, and AYQ25-7 pegmatites are dikes that cut the host rock foliation (Figure 1c). Pegmatite 213-1 is composed of several lenses which are concordant with the host rock foliation and show large grain size (crystals are several cm in length). This pegmatite, in particular, has geological features typical of a migmatite (Mehnert, 1968): the limits between the pegmatite body and the host rock are gradual and no zonation is observed within the pegmatite lenses.

ANALYTICAL METHODS

The seven studied samples (each of 5 – 10 kg) were collected from potential zircon bearing portions of the aforementioned pegmatites. They were crushed in the laboratory and heavy minerals were separated using a Wilfley table and a Frantz[®] magnetic separator. Zircons were extracted from the residual non-magnetic fraction. For each sample 100 zircon grains were randomly selected under a binocular microscope,

mounted in epoxy resin and then polished. The intra-grain compositional zoning was identified by cathodoluminescence (CL), using an ELM 3R luminoscope; and images were collected prior to analysis. Most grains preserve a number of subdomains of distinct composition that imply multiple igneous or metamorphic growth events.

Samples were dated by the U-Pb method using a Resonetics M50 workstation coupled to a Thermo X series II quadrupole ICP-MS at the Laboratorio de Estudios Isotópicos (LEI), Centro de Geociencias, UNAM, following the methodology reported in Solari *et al.* (2010).

The analytical data were filtered by discordance: results which yielded more than 10% or less than -5% of discordance were considered unreliable and were eliminated. Raw data were reduced using Iolite (Paton *et al.*, 2010) and the Vizual Age data reduction scheme (Petrus and Kamber, 2012), whereas all the Concordia plots were obtained, using Isoplot v. 3.70 software (Ludwig, 2008).

Trace elements (REE, Y and Hf) were collected from all zircons during U-Pb isotopic analysis. REE patterns were normalized to the chondrite values of McDonough and Sun (1995).

The size of Cerium and Europium anomalies was calculated from measured REE concentrations, using the following formulas: $Ce_{\text{anomaly}} = Ce/Ce^*$, where Ce is the chondrite-normalized Ce concentration and Ce^* is the average of the chondrite-normalized La and Pr; $Eu_{\text{anomaly}} = Eu/Eu^*$, where Eu is the chondrite-normalized Eu concentration and Eu^* is the average of the chondrite-normalized Sm and Gd concentrations.

The ages of each sample and the concentrations of Y, REE, Hf, Th, and U are shown in Table 1 and 2.

RESULTS

A detailed description of the seven pegmatite bodies sampled and the obtained analytical data (age and chemistry) is given in this section. The coordinates (latitude/longitude) of the pegmatite locations are shown in Table 3.

La Ofelia pegmatite

This is a discordant pegmatite body approximately 150 m wide and 300 m long, showing gradual grain size decrease towards the host quartzo-feldspathic gneiss. It is composed of three main zones: a pure phlogopite core, a phlogopite-clinopyroxene intermediate zone, and an external quartz-feldspar zone. The intermediate zone is represented by diopside highly altered to epidote and by phlogopite altered to chlorite. The external zone is made up of perthitic crystals of microcline with andesine-oligoclase highly altered to sericite and quartz. This zone has the largest abundance of accessory phases, such as apatite, zircon, titanite, and monazite. The zircon sample was taken from the external zone and, in spite of the metamorphic overprint it seems that the zircon crystals grew in the early stage of the pegmatite formation. During this work 500 μ m fragments of the fractured pink to purple colored subhedral zircon megacrysts were analyzed. Most of them have inherited cores and metamorphic rims in CL images. Overall 17 spots were analyzed from the core zones and 11 spots were analyzed from rims. Two distinct isotopic populations emerge from the data (Figure 2a). Cores yielded ages ranging from 1091 to 1367 Ma, whereas rims yield ages ranging from 969 to 1045 Ma. Most U-Pb ages are concordant. A mean age of 1190 ± 7 Ma (MSWD = 0.79) was calculated for core spots and a mean age of 991 ± 12 Ma (MSWD = 1.8) was obtained for rims (Figures 2a and 2c). Trace element concentrations in zircon cores are similar to zircon rims. La Ofelia zircons display moderate Hf (avg = 13123 ppm) and dispersed Y (496 to 2194 ppm; avg = 825) concentrations. The Th/U ratios range

Table 1. Zircon U-Pb dating results obtained from the Oaxacan pegmatites.

	CONCENTRATIONS				CORRECTED RATIOS*				CORRECTED AGES (Ma)				Disc (%)						
	U	Th	Th/U	²⁰⁷ Pb/ ²⁰⁶ Pb	$\pm 2\sigma$ abs	²⁰⁷ Pb/ ²³⁵ U	$\pm 2\sigma$ abs	²⁰⁶ Pb/ ²³⁸ U	$\pm 2\sigma$	²⁰⁷ Pb/ ²³⁵ U	$\pm 2\sigma$	²⁰⁷ Pb/ ²⁰⁶ Pb		$\pm 2\sigma$	Best age (Ma)				
	(ppm)*	(ppm)*																	
La Ofelia																			
<i>rim</i> s																			
La_Ofelia_1	49.3	40.9	0.83	0.0734	0.003	1.735	0.081	0.1686	0.004	0.21456	1004	25	1018	30	1066	59	1004	25	1.38
La_Ofelia_6	53.0	50.7	0.96	0.0779	0.005	1.760	0.110	0.1621	0.004	0.39482	969	22	1027	38	1229	76	969	22	5.65
La_Ofelia_7	66.2	51.0	0.77	0.0732	0.004	1.655	0.083	0.1650	0.005	0.54381	984	25	988	31	1082	53	984	25	0.40
La_Ofelia_13	61.3	53.5	0.87	0.0746	0.004	1.710	0.110	0.1693	0.004	0.22868	1008	24	1007	38	1063	61	1008	24	-0.10
La_Ofelia_14	77.7	67.0	0.86	0.0747	0.004	1.681	0.089	0.1649	0.005	0.08019	984	26	997	34	1050	63	984	26	1.30
La_Ofelia_15	56.2	50.8	0.90	0.0726	0.004	1.693	0.091	0.1687	0.004	0.00386	1005	25	1001	36	1009	75	1005	25	-0.40
La_Ofelia_16	106.5	69.0	0.65	0.0744	0.003	1.805	0.069	0.1760	0.004	0.20397	1045	23	1055	24	1076	51	1045	23	0.95
La_Ofelia_17	48.6	46.6	0.96	0.0745	0.005	1.710	0.120	0.1689	0.005	0.15408	1006	25	1016	40	1141	70	1006	25	0.98
La_Ofelia_23	49.4	48.9	0.99	0.0747	0.004	1.646	0.086	0.1639	0.004	0.15726	981	25	989	34	1051	62	981	25	0.81
La_Ofelia_27	49.6	43.8	0.88	0.0729	0.004	1.702	0.087	0.1690	0.005	0.52091	1007	25	1005	33	1045	63	1007	25	-0.20
La_Ofelia_29	58.6	54.0	0.92	0.0708	0.004	1.599	0.092	0.1623	0.004	0.42835	970	23	965	34	950	52	970	23	-0.52
<i>cores</i>																			
La_Ofelia_2	66.4	43.3	0.65	0.0812	0.004	2.300	0.110	0.2059	0.005	0.22367	1207	29	1213	34	1246	53	1246	53	0.49
La_Ofelia_3	197.0	137.6	0.70	0.0763	0.003	1.996	0.061	0.1895	0.005	0.81156	1119	25	1118	21	1107	36	1119	25	-0.09
La_Ofelia_4	160.9	50.7	0.32	0.0786	0.003	2.200	0.071	0.2016	0.005	0.14846	1186	25	1180	22	1186	30	1186	25	-0.51
La_Ofelia_5	51.8	35.2	0.68	0.0854	0.005	2.420	0.120	0.2018	0.005	0.51966	1185	28	1243	33	1367	56	1367	56	4.67
La_Ofelia_8	133.3	54.5	0.41	0.0795	0.003	2.179	0.074	0.2007	0.005	0.11860	1179	26	1173	24	1182	39	1179	26	-0.51
La_Ofelia_9	64.2	41.5	0.65	0.0816	0.004	2.250	0.110	0.2020	0.005	0.51643	1186	27	1202	36	1229	54	1229	54	1.33
La_Ofelia_10	76.1	42.8	0.56	0.0805	0.004	2.300	0.110	0.2057	0.005	0.17091	1206	26	1207	34	1176	53	1206	26	0.08
La_Ofelia_11	147.7	48.2	0.33	0.0805	0.003	2.189	0.077	0.1988	0.005	0.07349	1169	25	1176	24	1203	31	1169	25	0.60
La_Ofelia_12	203.0	94.6	0.47	0.0814	0.002	2.236	0.070	0.2032	0.005	0.33743	1192	27	1191	22	1212	23	1212	23	-0.08
La_Ofelia_18	58.0	55.2	0.95	0.0823	0.005	2.260	0.120	0.2018	0.006	0.15530	1185	29	1200	37	1256	62	1256	62	1.25
La_Ofelia_19	197.1	93.8	0.48	0.0777	0.003	2.107	0.091	0.1943	0.005	0.60774	1145	27	1149	29	1125	49	1145	27	0.35
La_Ofelia_20	88.4	32.4	0.37	0.0811	0.003	2.260	0.085	0.2056	0.005	0.32652	1205	29	1198	26	1220	38	1220	38	-0.58
La_Ofelia_24	152.8	64.4	0.42	0.0792	0.003	2.195	0.077	0.2029	0.005	0.68843	1191	26	1178	24	1179	42	1191	26	-1.10
La_Ofelia_25	78.5	43.5	0.55	0.0806	0.004	2.204	0.096	0.2011	0.005	0.45529	1181	28	1179	30	1225	47	1225	47	-0.17
La_Ofelia_26	150.4	70.9	0.47	0.0759	0.003	1.929	0.067	0.1845	0.005	0.71783	1091	25	1090	23	1076	50	1091	25	-0.09
La_Ofelia_28	131.0	56.2	0.43	0.0815	0.003	2.273	0.074	0.2053	0.005	0.03306	1204	26	1203	22	1244	34	1244	34	-0.08
La_Ofelia_30	53.6	38.2	0.71	0.0773	0.004	2.003	0.093	0.1880	0.005	0.58427	1114	28	1118	32	1130	57	1114	28	0.36
La Panchita																			
Zircon_21_PAN2	201.7	136.9	0.68	0.0717	0.002	1.644	0.089	0.1668	0.004	0.39572	994	21	992	34	989	37	994	21	-0.23
Zircon_22	233.0	156.5	0.67	0.0720	0.002	1.634	0.089	0.1644	0.004	0.27011	981	21	983	34	991	38	981	21	0.20
Zircon_23	231.1	155.8	0.67	0.0712	0.003	1.627	0.094	0.1651	0.004	0.37741	985	20	979	36	970	48	985	20	-0.62
Zircon_24	236.3	159.3	0.67	0.0692	0.002	1.581	0.088	0.1667	0.004	0.40954	994	21	964	36	921	47	994	21	-3.12

*U and Th concentrations are calculated employing an external standard zircon as in Paton et al., 2010, Geochemistry, Geophysics, Geosystems. *²⁰⁷Pb/²⁰⁶Pb ratios, ages and errors are calculated according to Petrus and Kamber, 2012, Geostandards Geoanalytical Research.

continues

Table 1 (cont.). Zircon U-Pb dating results obtained from the Oaxacan pegmatites.

	CONCENTRATIONS				CORRECTED RATIOS*				CORRECTED AGES (Ma)				Disc (%)						
	U (ppm)*	Th (ppm)*	Th/U	²⁰⁷ Pb/ ²⁰⁶ Pb	$\pm 2\sigma$ abs	²⁰⁷ Pb/ ²³⁵ U	$\pm 2\sigma$ abs	²⁰⁶ Pb/ ²³⁸ U	$\pm 2\sigma$	Rho	²⁰⁶ Pb/ ²³⁸ U	$\pm 2\sigma$		²⁰⁷ Pb/ ²⁰⁶ Pb	$\pm 2\sigma$	Best age (Ma)			
La Panchita (cont.)																			
Zircon_25	257.0	174.5	0.68	0.0717	0.003	1.657	0.095	0.1686	0.004	0.02482	1005	21	991	37	964	43	1005	21	-1.37
Zircon_26	213.7	143.9	0.67	0.0719	0.002	1.657	0.091	0.1676	0.004	0.19820	999	21	991	35	969	38	999	21	-0.80
Zircon_27	249.0	169.2	0.68	0.0723	0.002	1.644	0.088	0.1657	0.004	0.29679	989	21	987	34	992	32	989	21	-0.15
Zircon_28	248.4	168.8	0.68	0.0703	0.002	1.586	0.087	0.1655	0.004	0.04604	987	20	966	33	919	42	987	20	-2.18
Zircon_29	214.2	81.0	0.38	0.0707	0.002	1.557	0.086	0.1597	0.004	0.08892	955	20	952	34	935	42	955	20	-0.34
Zircon_30_PAN2	261.8	176.7	0.67	0.0707	0.002	1.616	0.087	0.1676	0.004	0.24405	999	21	978	32	966	40	999	21	-2.12
Zircon_31_PAN3	164.1	68.9	0.42	0.0707	0.002	1.583	0.089	0.1637	0.004	0.30212	977	21	965	34	950	45	977	21	-1.27
Zircon_32	203.2	85.6	0.42	0.0713	0.003	1.594	0.091	0.1620	0.004	0.03324	968	20	966	36	971	46	968	20	-0.18
Zircon_33	211.5	91.9	0.43	0.0703	0.003	1.556	0.087	0.1616	0.004	0.40950	965	20	952	35	943	38	965	20	-1.41
Zircon_34	185.7	79.1	0.43	0.0708	0.003	1.631	0.094	0.1687	0.004	0.23761	1005	21	981	36	927	44	1005	21	-2.45
Zircon_35	239.1	99.7	0.42	0.0722	0.003	1.620	0.093	0.1647	0.004	0.40190	983	21	980	34	965	39	983	21	-0.29
Zircon_36	197.5	79.7	0.40	0.0707	0.002	1.544	0.087	0.1612	0.004	0.17365	964	20	947	35	946	35	964	20	-1.75
Zircon_37	260.3	101.5	0.39	0.0698	0.002	1.547	0.085	0.1609	0.004	0.07872	962	20	948	34	937	37	962	20	-1.43
Zircon_38	216.0	92.3	0.43	0.0703	0.002	1.596	0.089	0.1658	0.004	0.09966	989	21	970	34	949	34	989	21	-1.95
Zircon_39	262.9	110.6	0.42	0.0717	0.003	1.608	0.093	0.1630	0.004	0.23326	974	20	972	36	974	41	974	20	-0.15
Zircon_40_PAN3	340.0	140.9	0.41	0.0718	0.002	1.591	0.086	0.1615	0.004	0.06893	965	20	966	34	968	33	965	20	0.09
AYQ25-7																			
Zircon_02	73.9	43.9	0.59	0.0737	0.005	1.590	0.110	0.1592	0.004	0.20034	952	20	960	31	1005	74	952	20	0.83
Zircon_03	142.5	126.3	0.89	0.0714	0.003	1.533	0.061	0.1569	0.004	0.02015	939	21	942	25	978	44	939	21	0.32
Zircon_04	96.7	60.8	0.63	0.0720	0.003	1.568	0.082	0.1586	0.004	0.44083	949	24	955	33	1001	43	949	24	0.63
Zircon_05	102.4	61.8	0.60	0.0732	0.003	1.563	0.083	0.1598	0.003	0.24487	955	19	961	30	1002	38	955	19	0.62
Zircon_08	69.4	41.9	0.60	0.0719	0.004	1.520	0.110	0.1554	0.004	0.34679	931	21	936	40	970	72	931	21	0.53
Zircon_13	60.3	34.0	0.56	0.0679	0.004	1.520	0.090	0.1596	0.004	0.16485	954	23	933	35	864	59	954	23	-2.25
Zircon_14	76.0	46.6	0.61	0.0710	0.004	1.566	0.087	0.1581	0.003	0.00170	946	18	958	33	1005	59	946	18	1.25
Zircon_15	90.9	55.8	0.61	0.0765	0.004	1.673	0.089	0.1598	0.004	0.44375	956	20	1005	34	1068	57	956	20	4.88
Zircon_16	76.0	46.0	0.61	0.0718	0.004	1.571	0.086	0.1599	0.004	0.12165	956	19	961	33	983	57	956	19	0.52
Zircon_17	147.2	123.1	0.84	0.0724	0.003	1.596	0.074	0.1600	0.003	0.55708	957	18	967	29	1014	56	957	18	1.03
Zircon_18	148.3	106.6	0.72	0.0797	0.004	1.764	0.094	0.1602	0.004	0.19327	958	22	1029	35	1228	50	958	22	6.90
Zircon_20	52.6	30.1	0.57	0.0715	0.003	1.628	0.089	0.1639	0.004	0.05846	978	21	979	33	971	57	978	21	0.10
Zircon_21	65.7	42.1	0.64	0.0734	0.003	1.625	0.075	0.1623	0.004	0.14537	969	23	978	28	1046	47	969	23	0.92
Zircon_22	120.2	94.0	0.78	0.0735	0.003	1.626	0.069	0.1630	0.004	0.25963	973	20	978	26	1038	48	973	20	0.51
Zircon_23	71.2	39.6	0.56	0.0733	0.004	1.647	0.094	0.1643	0.004	0.64425	981	20	987	33	1032	74	981	20	0.61
Zircon_24	86.9	48.0	0.55	0.0724	0.003	1.637	0.076	0.1641	0.004	0.50888	979	22	983	29	988	35	979	22	0.41
Zircon_25	94.5	57.9	0.61	0.0721	0.003	1.641	0.079	0.1679	0.004	0.27911	1000	20	984	30	996	41	1000	20	-1.63

*U and Th concentrations are calculated employing an external standard zircon as in Paton *et al.*, 2010. Geochemistry, Geophysics, Geosystems. *²⁰⁷Pb/²⁰⁶Pb ratios, ages and errors are calculated according to Petrus and Kamber, 2012, Geostandards Geoanalytical Research.

continues

Table 1 (cont.). Zircon U-Pb dating results obtained from the Oaxacan pegmatites.

	CONCENTRATIONS				CORRECTED RATIOS*								CORRECTED AGES (Ma)						
	U	Th	Th/U	²⁰⁷ Pb/ ²⁰⁶ Pb	$\pm 2\sigma$ abs	²⁰⁷ Pb/ ²³⁵ U	$\pm 2\sigma$ abs	²⁰⁶ Pb/ ²³⁸ U	$\pm 2\sigma$ abs	Rho	²⁰⁶ Pb/ ²³⁸ U	$\pm 2\sigma$	²⁰⁷ Pb/ ²³⁵ U	$\pm 2\sigma$	²⁰⁷ Pb/ ²⁰⁶ Pb	$\pm 2\sigma$	Best age (Ma)	$\pm 2\sigma$	Disc (%)
	(ppm) [†]	(ppm) [†]																	
AVQ25-7 (cont.)																			
Zircon_26	59.5	33.2	0.56	0.0707	0.003	1.609	0.088	0.1613	0.004	0.45342	964	22	972	33	1011	43	964	22	0.82
Zircon_27	64.1	36.6	0.57	0.0739	0.003	1.690	0.076	0.1658	0.004	0.29157	989	21	1003	27	1015	39	989	21	1.40
Zircon_28	77.5	44.0	0.57	0.0708	0.004	1.581	0.089	0.1616	0.003	0.36276	966	18	961	33	939	60	966	18	-0.52
Zircon_29	74.2	45.6	0.61	0.0727	0.003	1.602	0.086	0.1615	0.004	0.22703	965	21	981	34	984	47	965	21	1.63
Zircon_30	91.0	55.6	0.61	0.0737	0.004	1.633	0.090	0.1601	0.004	0.08985	957	23	979	34	1017	58	957	23	2.25
Zircon_31	69.1	39.1	0.57	0.0795	0.004	1.820	0.100	0.1641	0.004	0.35592	979	22	1061	38	1199	67	979	22	7.73
176-1																			
<i> rims</i>																			
D_176_1_1	257.0	117.2	0.46	0.0731	0.002	1.629	0.053	0.1609	0.004	0.72589	962	21	981	20	1009	42	962	21	1.94
D_176_1_2	227.0	99.2	0.44	0.0737	0.003	1.646	0.062	0.1636	0.004	0.64910	977	22	1001	21	1003	36	977	22	2.40
D_176_1_4	256.0	149.4	0.58	0.0702	0.002	1.593	0.060	0.1621	0.004	0.46179	968	21	969	24	954	36	968	21	0.10
D_176_1_5	326.1	121.0	0.37	0.0709	0.003	1.656	0.057	0.1652	0.004	0.48196	986	24	995	24	966	34	986	24	0.90
D_176_1_6	158.4	55.9	0.35	0.0719	0.003	1.652	0.068	0.1649	0.004	0.07887	984	23	988	26	988	46	984	23	0.40
D_176_1_7	186.0	72.6	0.39	0.0724	0.003	1.638	0.059	0.1649	0.004	0.67344	985	23	984	23	1004	59	985	23	-0.10
D_176_1_9	209.0	76.9	0.37	0.0716	0.003	1.582	0.054	0.1612	0.004	0.24479	963	24	961	21	981	30	963	24	-0.21
D_176_1_10	167.0	67.5	0.40	0.0705	0.003	1.640	0.062	0.1665	0.004	0.17350	993	23	984	23	970	51	993	23	-0.91
D_176_1_11	145.9	59.9	0.41	0.0730	0.003	1.676	0.065	0.1658	0.004	0.26477	989	23	1002	23	1008	55	989	23	1.30
D_176_1_12	158.0	51.9	0.33	0.0736	0.003	1.638	0.083	0.1639	0.005	0.42632	978	25	982	30	998	41	978	25	0.41
D_176_1_13	288.0	203.7	0.71	0.0713	0.003	1.630	0.056	0.1640	0.004	0.35964	979	22	981	23	969	38	979	22	0.20
D_176_1_14	159.7	61.3	0.38	0.0711	0.003	1.607	0.059	0.1643	0.004	0.28990	981	22	979	22	954	39	981	22	-0.20
D_176_1_15	223.0	99.7	0.45	0.0718	0.003	1.625	0.060	0.1610	0.004	0.51998	962	21	978	24	985	44	962	21	1.64
D_176_1_16	275.0	180.0	0.65	0.0720	0.002	1.635	0.057	0.1654	0.004	0.29256	987	23	985	21	963	44	987	23	-0.20
D_176_1_17	140.0	52.0	0.37	0.0728	0.003	1.664	0.068	0.1662	0.004	0.11183	991	23	993	26	995	50	991	23	0.20
D_176_1_19	248.0	118.1	0.48	0.0717	0.002	1.647	0.050	0.1645	0.004	0.23980	982	21	988	19	972	38	982	21	0.61
D_176_1_20	197.9	105.1	0.53	0.0730	0.003	1.630	0.064	0.1593	0.004	0.09033	953	21	980	25	1022	58	953	21	2.76
D_176_1_21	520.0	149.7	0.29	0.0712	0.002	1.632	0.057	0.1624	0.004	0.89255	970	25	981	24	974	42	970	25	1.12
D_176_1_22	177.0	61.4	0.35	0.0731	0.003	1.654	0.084	0.1626	0.005	0.40562	971	28	989	31	1044	51	971	28	1.82
D_176_1_23	284.0	163.7	0.58	0.0737	0.002	1.707	0.052	0.1644	0.004	0.33479	983	22	1010	20	1024	38	983	22	2.67
D_176_1_24	270.7	172.8	0.64	0.0727	0.002	1.647	0.053	0.1645	0.004	0.32931	982	22	987	20	1021	44	982	22	0.51
D_176_1_25	173.3	72.9	0.42	0.0710	0.003	1.621	0.060	0.1634	0.004	0.21159	976	22	977	23	951	33	976	22	0.10
D_176_1_28	382.0	210.5	0.55	0.0722	0.002	1.624	0.057	0.1634	0.004	0.47986	976	21	978	23	989	39	976	21	0.20
<i> cores</i>																			
D_176_1_3	1175.0	88.7	0.08	0.0775	0.002	2.121	0.056	0.1965	0.005	0.45806	1156	24	1156	18	1128	40	1156	24	0.00
D_176_1_8	212.0	99.6	0.47	0.0795	0.003	2.107	0.066	0.1923	0.005	0.32652	1134	25	1151	21	1194	26	1134	25	1.48
183-2																			
A_183_2_1	137.0	65.1	0.48	0.0738	0.004	1.597	0.077	0.1609	0.004	0.16998	962	21	974	29	1030	42	962	21	1.23
A_183_2_2	162.0	129.5	0.80	0.0733	0.003	1.565	0.047	0.1566	0.004	0.15813	938	20	956	19	1012	42	938	20	1.88

*U and Th concentrations are calculated employing an external standard zircon as in Paton *et al.*, 2010, Geochemistry, Geophysics, Geosystems. *²⁰⁷Pb/²⁰⁶Pb ratios, ages and errors are calculated according to Petrus and Kamber, 2012, Geostandards Geoanalytical Research.

continues

Table 1 (cont.). Zircon U-Pb dating results obtained from the Oaxacan pegmatites.

	CONCENTRATIONS				CORRECTED RATIOS*				CORRECTED AGES (Ma)				Disc (%)						
	U (ppm) [†]	Th (ppm) [†]	Th/U	²⁰⁷ Pb/ ²⁰⁶ Pb	$\pm 2\sigma$ abs	²⁰⁷ Pb/ ²³⁵ U	$\pm 2\sigma$	²⁰⁶ Pb/ ²³⁸ U	$\pm 2\sigma$ abs	Rho	²⁰⁶ Pb/ ²³⁸ U	$\pm 2\sigma$		²⁰⁷ Pb/ ²³⁵ U	$\pm 2\sigma$	²⁰⁷ Pb/ ²⁰⁶ Pb	$\pm 2\sigma$	Best age (Ma)	$\pm 2\sigma$
183-2 (cont.)																			
A_183_2_3	167.2	82.4	0.49	0.0722	0.003	1.592	0.060	0.1627	0.004	0.19556	972	22	974	24	1002	48	972	22	0.21
A_183_2_4	179.4	92.4	0.52	0.0731	0.003	1.626	0.067	0.1630	0.004	0.45416	973	21	978	25	1022	30	973	21	0.51
A_183_2_5	99.6	46.6	0.47	0.0745	0.004	1.639	0.078	0.1634	0.004	0.25619	976	23	997	27	1073	50	976	23	2.11
A_183_2_7	131.1	77.8	0.59	0.0714	0.003	1.562	0.064	0.1609	0.004	0.29248	962	21	959	26	986	45	962	21	-0.31
A_183_2_8	154.0	80.5	0.52	0.0717	0.003	1.607	0.062	0.1653	0.004	0.36557	986	22	971	26	967	39	986	22	-1.54
A_183_2_9	126.5	93.8	0.74	0.0728	0.003	1.628	0.066	0.1656	0.004	0.61071	988	22	979	25	1039	48	988	22	-0.92
A_183_2_10	75.2	39.0	0.52	0.0735	0.004	1.638	0.092	0.1632	0.004	0.06864	975	24	987	33	1080	68	975	24	1.22
A_183_2_11	182.0	85.5	0.47	0.0733	0.003	1.594	0.053	0.1606	0.004	0.12327	960	22	967	21	1014	45	960	22	0.72
A_183_2_12	130.2	100.9	0.77	0.0720	0.003	1.626	0.065	0.1661	0.004	0.60242	991	22	978	25	980	50	991	22	-1.33
A_183_2_13	187.8	132.1	0.70	0.0715	0.003	1.552	0.056	0.1597	0.004	0.11036	955	22	950	22	976	42	955	22	-0.53
A_183_2_14	121.1	56.2	0.46	0.0762	0.004	1.683	0.082	0.1608	0.004	0.40447	961	23	1004	31	1113	62	961	23	4.28
A_183_2_15	211.5	144.8	0.68	0.0695	0.003	1.533	0.048	0.1596	0.004	0.36219	954	21	942	19	936	46	954	21	-1.27
A_183_2_16	259.0	183.0	0.71	0.0756	0.003	1.667	0.055	0.1645	0.004	0.06362	982	21	995	21	1091	48	982	21	1.31
A_183_2_17	141.0	73.3	0.52	0.0742	0.003	1.612	0.059	0.1618	0.004	0.67545	966	22	974	23	1034	43	966	22	0.82
A_183_2_18	205.0	168.7	0.82	0.0704	0.002	1.551	0.048	0.1592	0.004	0.39450	952	21	950	19	951	37	952	21	-0.21
A_183_2_19	140.2	95.1	0.68	0.0715	0.003	1.574	0.067	0.1615	0.004	0.03920	965	22	958	26	962	40	965	22	-0.73
A_183_2_20	152.6	69.7	0.46	0.0734	0.003	1.556	0.070	0.1594	0.004	0.30654	954	22	957	29	1026	42	954	22	0.31
A_183_2_21	122.6	61.0	0.50	0.0740	0.004	1.642	0.084	0.1670	0.004	0.04381	995	23	990	31	1023	40	995	23	-0.51
A_183_2_22	117.0	95.7	0.82	0.0747	0.003	1.603	0.070	0.1612	0.004	0.35381	963	22	973	26	1073	41	963	22	1.03
A_183_2_23	143.0	114.0	0.80	0.0802	0.004	1.748	0.070	0.1593	0.004	0.14128	953	21	1025	25	1202	47	953	21	7.02
A_183_2_24	193.7	156.4	0.81	0.0720	0.003	1.610	0.056	0.1640	0.004	0.26828	979	21	973	22	992	40	979	21	-0.62
A_183_2_25	112.6	81.5	0.72	0.0738	0.003	1.586	0.062	0.1600	0.004	0.10936	957	22	963	24	1015	61	957	22	0.62
A_183_2_26	121.3	88.0	0.73	0.0734	0.003	1.577	0.058	0.1618	0.004	0.65537	967	22	960	23	986	51	967	22	-0.73
A_183_2_27	239.0	150.0	0.63	0.0724	0.003	1.624	0.056	0.1654	0.004	0.71886	987	22	981	22	994	39	987	22	-0.61
A_183_2_28	170.3	105.8	0.62	0.0725	0.003	1.628	0.072	0.1656	0.004	0.57347	988	23	983	28	1022	45	988	23	-0.51
A_183_2_29	189.0	180.0	0.95	0.0738	0.003	1.600	0.053	0.1612	0.004	0.10993	963	22	969	22	1061	46	963	22	0.62
A_183_2_30	256.0	124.4	0.49	0.0712	0.002	1.568	0.052	0.1629	0.004	0.27586	973	22	957	20	970	47	973	22	-1.67
A_183_2_31	166.0	148.0	0.89	0.0718	0.003	1.583	0.059	0.1605	0.004	0.06038	960	22	962	24	984	47	960	22	0.21
A_183_2_32	139.1	88.8	0.64	0.0719	0.003	1.605	0.066	0.1644	0.004	0.59168	981	22	975	27	1002	45	981	22	-0.62
A_183_2_33	121.5	71.2	0.59	0.0748	0.003	1.683	0.066	0.1631	0.004	0.64102	974	23	1000	25	1077	42	974	23	2.60
213-1																			
C_213_1_1	115.9	64.7	0.56	0.0722	0.004	1.608	0.085	0.1629	0.004	0.16614	973	22	970	32	1015	56	973	22	-0.31
C_213_1_2	113.8	71.3	0.63	0.0727	0.003	1.665	0.067	0.1663	0.004	0.62762	991	23	994	25	1015	49	991	23	0.30
C_213_1_3	100.0	63.0	0.63	0.0724	0.003	1.659	0.063	0.1672	0.004	0.03338	997	24	995	24	1001	36	997	24	-0.20
C_213_1_4	163.0	140.0	0.86	0.0717	0.003	1.587	0.071	0.1620	0.005	0.32156	968	28	963	27	975	45	968	28	-0.52
C_213_1_5	79.6	39.1	0.49	0.0728	0.004	1.652	0.091	0.1637	0.004	0.12948	977	25	986	34	1047	60	977	25	0.91

* U and Th concentrations are calculated employing an external standard zircon as in Paton *et al.*, 2010, Geochemistry, Geophysics, Geosystems. * ²⁰⁷Pb/²⁰⁶Pb ratios, ages and errors are calculated according to Petrus and Kamber, 2012, Geostandards Geoanalytical Research.

continues

Table 1 (cont.). Zircon U-Pb dating results obtained from the Oaxacan pegmatites.

	CONCENTRATIONS				CORRECTED RATIOS*				CORRECTED AGES (Ma)				Disc (%)						
	U (ppm) [†]	Th (ppm) [‡]	Th/U	²⁰⁷ Pb/ ²⁰⁶ Pb	$\pm 2\sigma$ abs	²⁰⁷ Pb/ ²³⁵ U	$\pm 2\sigma$ abs	²⁰⁶ Pb/ ²³⁸ U	$\pm 2\sigma$ abs	²⁰⁶ Pb/ ²³⁸ U	$\pm 2\sigma$	²⁰⁷ Pb/ ²⁰⁶ Pb		$\pm 2\sigma$	Best age (Ma)	$\pm 2\sigma$			
213-1 (cont.)																			
C_213_1_6	141.2	119.5	0.85	0.0712	0.003	1.638	0.062	0.1649	0.004	0.40989	984	21	983	24	954	35	984	21	-0.10
C_213_1_8	82.3	44.4	0.54	0.0712	0.003	1.621	0.072	0.1632	0.004	0.26863	975	24	976	28	958	48	975	24	0.10
C_213_1_9	137.0	109.0	0.80	0.0734	0.003	1.710	0.066	0.1655	0.004	0.15834	987	21	1014	26	1062	43	987	21	2.66
C_213_1_10	110.3	69.8	0.63	0.0733	0.003	1.652	0.071	0.1597	0.004	0.10910	955	21	988	28	1010	50	955	21	3.34
C_213_1_11	138.0	87.4	0.63	0.0722	0.003	1.579	0.081	0.1630	0.004	0.17856	977	24	960	30	963	59	977	24	-1.77
C_213_1_12	77.9	38.9	0.50	0.0734	0.004	1.646	0.075	0.1636	0.004	0.57684	977	24	986	29	1038	64	977	24	0.91
C_213_1_13	72.5	34.4	0.47	0.0737	0.004	1.717	0.082	0.1653	0.004	0.18726	986	23	1017	30	1068	65	986	23	3.05
C_213_1_15	91.4	52.1	0.57	0.0686	0.003	1.588	0.061	0.1615	0.004	0.64477	965	22	964	24	881	53	965	22	-0.10
C_213_1_16	111.3	54.0	0.49	0.0710	0.004	1.612	0.081	0.1640	0.004	0.49753	979	22	977	33	990	44	979	22	-0.20
C_213_1_17	88.3	51.4	0.58	0.0731	0.004	1.650	0.092	0.1632	0.004	0.12030	974	24	985	35	993	64	974	24	1.12
C_213_1_19	135.6	91.8	0.68	0.0734	0.003	1.640	0.064	0.1639	0.004	0.42125	978	22	984	25	989	42	978	22	0.61
C_213_1_20	127.7	81.4	0.64	0.0739	0.003	1.647	0.072	0.1644	0.004	0.42111	981	22	993	27	1014	56	981	22	1.21
C_213_1_21	86.1	41.8	0.49	0.0697	0.003	1.638	0.075	0.1704	0.005	0.17025	1014	25	990	29	949	45	1014	25	-2.42
C_213_1_22	140.2	92.2	0.66	0.0722	0.003	1.633	0.064	0.1632	0.004	0.29562	974	23	981	26	989	33	974	23	0.71
C_213_1_24	119.2	67.9	0.57	0.0729	0.003	1.716	0.073	0.1725	0.005	0.62685	1026	25	1012	27	1001	66	1026	25	-1.38
C_213_1_25	81.5	44.6	0.55	0.0726	0.003	1.785	0.079	0.1741	0.005	0.03209	1035	26	1037	29	1045	49	1035	26	0.19
C_213_1_27	161.0	101.0	0.63	0.0710	0.003	1.552	0.060	0.1546	0.004	0.25890	927	22	949	24	959	50	927	22	2.32
C_213_1_28	111.3	66.8	0.60	0.0732	0.003	1.689	0.089	0.1656	0.004	0.49277	988	24	1001	32	1046	74	988	24	1.30
C_213_1_29	91.4	44.2	0.48	0.0747	0.003	1.805	0.072	0.1743	0.005	0.05436	1035	27	1046	25	1086	43	1035	27	1.05
C_213_1_30	106.7	60.5	0.57	0.0719	0.002	1.623	0.057	0.1648	0.004	0.38615	983	23	978	22	987	46	983	23	-0.51
C_213_1_31	137.9	104.2	0.76	0.0716	0.003	1.631	0.066	0.1650	0.005	0.28780	985	25	985	24	977	45	985	25	0.00
C_213_1_32	124.0	77.5	0.63	0.0715	0.003	1.646	0.073	0.1644	0.004	0.41552	981	24	985	28	982	40	981	24	0.41
OC22-4AB																			
<i>rims</i>																			
Zircon_03	332.0	74.8	0.23	0.0711	0.002	1.601	0.065	0.1615	0.003	0.34291	965	17	970	20	976	32	965	17	0.52
Zircon_05	1346.0	111.0	0.08	0.0784	0.002	1.893	0.060	0.1723	0.003	0.17575	1025	17	1078	18	1155	32	1025	17	4.92
Zircon_10	1719.0	130.3	0.08	0.0715	0.002	1.657	0.053	0.1654	0.003	0.51876	987	17	992	19	978	30	987	17	0.50
Zircon_11	218.4	43.0	0.20	0.0774	0.002	1.872	0.071	0.1724	0.004	0.43143	1025	21	1071	24	1127	32	1025	21	4.30
Zircon_23	2290.0	229.0	0.10	0.0738	0.002	1.748	0.056	0.1726	0.004	0.74062	1026	19	1026	21	1031	31	1026	19	0.00
Zircon_30	202.4	36.4	0.18	0.0756	0.002	1.867	0.068	0.1803	0.004	0.54820	1069	20	1069	23	1090	34	1069	20	0.00
<i>cores</i>																			
Zircon_01_OC22-4a	1598.0	136.4	0.09	0.0798	0.002	2.177	0.068	0.1968	0.004	0.40325	1158	20	1173	22	1194	32	1158	20	1.28
Zircon_02	389.0	67.8	0.17	0.0746	0.002	2.005	0.075	0.1902	0.005	0.23343	1123	27	1117	26	1063	40	1123	27	-0.54
Zircon_04	1720.0	228.0	0.13	0.0785	0.002	2.234	0.073	0.2031	0.004	0.36890	1192	20	1192	22	1162	35	1192	20	0.00
Zircon_07	1765.0	165.5	0.09	0.0794	0.002	2.247	0.075	0.2021	0.004	0.50625	1187	21	1196	23	1184	30	1187	21	0.75
Zircon_08	1115.0	101.8	0.09	0.0810	0.002	2.243	0.073	0.1973	0.004	0.45179	1161	20	1194	23	1210	40	1161	20	2.76

*U and Th concentrations are calculated employing an external standard zircon as in Paton et al., 2010. Geochemistry, Geophysics, Geosystems. ²⁰⁷Pb/²⁰⁶Pb ratios, ages and errors are calculated according to Petrus and Kamber, 2012. Geostandards Geoanalytical Research.

continues

Table 1 (cont.). Zircon U-Pb dating results obtained from the Oaxacan pegmatites.

OC22-4AB cores (cont.)	CONCENTRATIONS					CORRECTED RATIOS*					CORRECTED AGES (Ma)								
	U	Th	Th/U	$^{207}\text{Pb}/^{206}\text{Pb}$	$\pm 2\sigma$ abs	$^{207}\text{Pb}/^{238}\text{U}$	$\pm 2\sigma$ abs	$^{206}\text{Pb}/^{238}\text{U}$	$\pm 2\sigma$ abs	Rho	$^{206}\text{Pb}/^{238}\text{U}$	$\pm 2\sigma$	$^{207}\text{Pb}/^{235}\text{U}$	$\pm 2\sigma$	Best age (Ma)	$\pm 2\sigma$	Disc (%)		
	(ppm)*	(ppm)*																	
Zircon_09	1212.0	101.4	0.08	0.0795	0.002	2.255	0.069	0.2011	0.004	0.25045	1181	19	1198	22	1186	28	1181	19	1.42
Zircon_12	1207.0	86.8	0.07	0.0793	0.002	2.230	0.070	0.2023	0.004	0.55016	1188	22	1190	22	1188	28	1188	22	0.17
Zircon_13	1390.0	134.9	0.10	0.0797	0.002	2.269	0.073	0.2049	0.004	0.34712	1201	20	1203	23	1197	32	1201	20	0.17
Zircon_14	988.0	74.9	0.08	0.0831	0.002	2.333	0.084	0.2038	0.004	0.54236	1196	22	1222	24	1267	32	1267	32	2.13
Zircon_15	1563.0	114.7	0.07	0.0800	0.002	2.216	0.075	0.1996	0.004	0.69076	1173	20	1186	23	1200	34	1173	20	1.10
Zircon_17	2260.0	219.0	0.10	0.0797	0.002	2.243	0.072	0.2033	0.004	0.53506	1193	23	1194	22	1188	22	1193	23	0.08
Zircon_19	2260.0	279.0	0.12	0.0795	0.002	2.232	0.072	0.2037	0.004	0.60093	1195	20	1191	22	1179	27	1195	20	-0.34
Zircon_20	1890.0	170.0	0.09	0.0794	0.002	2.236	0.069	0.2040	0.004	0.57698	1197	22	1192	22	1178	32	1197	22	-0.42
Zircon_21	2890.0	260.0	0.09	0.0794	0.002	2.266	0.071	0.2072	0.004	0.69554	1214	22	1202	23	1181	29	1214	22	-1.00
Zircon_22	2840.0	319.0	0.11	0.0801	0.002	2.289	0.069	0.2070	0.004	0.42522	1213	22	1209	20	1196	21	1196	21	-0.33
Zircon_24	2420.0	240.0	0.10	0.0793	0.002	2.236	0.072	0.2042	0.004	0.49204	1198	23	1192	22	1184	30	1198	23	-0.50
Zircon_25	1631.0	170.2	0.10	0.0819	0.002	2.327	0.075	0.2057	0.004	0.34982	1207	23	1221	22	1242	32	1242	32	1.15
Zircon_26	2150.0	208.0	0.10	0.0808	0.002	2.396	0.076	0.2144	0.005	0.65815	1252	24	1241	23	1216	32	1216	32	-0.89
Zircon_27	340.0	69.2	0.20	0.0796	0.002	2.125	0.082	0.1935	0.004	0.48241	1140	24	1162	26	1186	39	1140	24	1.89
Zircon_28	1990.0	194.0	0.10	0.0733	0.002	1.675	0.054	0.1656	0.003	0.60761	988	19	999	21	1018	24	988	19	1.10
Zircon_28_OC22-4B	1584.0	139.0	0.09	0.0801	0.002	2.259	0.079	0.2051	0.006	0.74706	1203	29	1199	24	1190	37	1203	29	-0.33
Zircon_29	1379.0	104.7	0.08	0.0803	0.002	2.304	0.074	0.2085	0.004	0.51505	1221	22	1213	22	1198	32	1198	32	-0.66
Zircon_31	1903.0	174.7	0.09	0.0801	0.002	2.305	0.074	0.2094	0.005	0.70383	1225	24	1214	22	1199	30	1199	30	-0.91
Zircon_32	1479.0	117.9	0.08	0.0789	0.002	2.219	0.074	0.2034	0.005	0.58014	1194	24	1187	22	1179	21	1194	24	-0.59
Zircon_33	1830.0	200.0	0.11	0.0820	0.004	2.421	0.087	0.2138	0.006	0.80661	1249	33	1249	25	1243	85	1243	85	0.00
Zircon_35	1895.0	245.7	0.13	0.0805	0.002	2.259	0.071	0.2041	0.004	0.50093	1197	22	1199	22	1206	32	1206	32	0.17
Zircon_36	1660.0	194.9	0.12	0.0796	0.002	2.285	0.078	0.2070	0.004	0.44005	1213	22	1208	23	1184	28	1213	22	-0.41
Zircon_37	472.0	36.1	0.08	0.0816	0.002	2.436	0.081	0.2169	0.004	0.19729	1265	23	1253	24	1228	32	1228	32	-0.96
Zircon_38	2140.0	233.0	0.11	0.0797	0.002	2.221	0.071	0.2026	0.004	0.30487	1189	22	1187	22	1201	28	1189	22	-0.17
Zircon_40	1828.0	252.0	0.14	0.0807	0.002	2.294	0.074	0.2070	0.004	0.78618	1213	22	1210	22	1209	33	1209	33	-0.25
Zircon_41	2451.0	321.0	0.13	0.0812	0.002	2.319	0.072	0.2079	0.005	0.63260	1217	25	1218	22	1222	33	1222	33	0.08
Zircon_42	1639.0	150.9	0.09	0.0802	0.002	2.292	0.073	0.2065	0.005	0.75156	1210	24	1210	22	1205	34	1205	34	0.00
Zircon_43	1663.0	139.5	0.08	0.0796	0.002	2.233	0.072	0.2044	0.005	0.40489	1199	24	1191	23	1184	32	1199	24	-0.67
Zircon_44	1820.0	173.5	0.10	0.0807	0.002	2.305	0.073	0.2080	0.004	0.56894	1218	22	1214	22	1213	24	1213	24	-0.33
Zircon_45	693.0	45.9	0.07	0.0776	0.002	2.058	0.073	0.1918	0.005	0.47874	1131	25	1135	23	1144	29	1131	25	0.35
Zircon_46	1603.0	166.5	0.10	0.0796	0.002	2.266	0.074	0.2065	0.004	0.53234	1210	23	1202	22	1188	28	1210	23	-0.67
Zircon_47	1353.0	122.7	0.09	0.0799	0.002	2.276	0.077	0.2081	0.005	0.35058	1219	26	1205	23	1195	36	1195	36	-1.16
Zircon_49	1407.0	148.7	0.11	0.0799	0.002	2.275	0.076	0.2061	0.004	0.79108	1208	21	1204	20	1198	33	1198	33	-0.33
Zircon_50	1790.0	175.5	0.10	0.0801	0.002	2.245	0.069	0.2039	0.004	0.45930	1196	21	1195	22	1198	35	1196	21	-0.08

*U and Th concentrations are calculated employing an external standard zircon as in Paton *et al.*, 2010. Geochemistry, Geophysics, Geosystems. ²⁰⁷Pb/²⁰⁶Pb ratios, ages and errors are calculated according to Petrus and Kamber, 2012, Geostandards Geoanalytical Research.

from 0.32 to 0.99, and this variation is independent of age. The analyzed zircons have uniform REE characteristics (Figure 2b), with a significant enrichment in HREE (Lu_N/La_N avg = 4325), well-defined positive Ce/Ce^* (avg = 21.3) and negative Eu/Eu^* (avg = 0.20) anomalies. HREE enrichment measured by the ratio Lu_N/Gd_N gives an average of 23.9 and for LREE the Sm_N/La_N ratio averages 54.

La Panchita pegmatite

La Panchita pegmatite consists of several pegmatite lenses located inside of an extensional pyroxenitic dike. During the present work only one pegmatite lens was studied. This pegmatite body measures 2 – 4 m across and up to 10 m long and intrudes into a large (more than 200 m across and some kilometers long) pyroxenite dike that in turn is intruding the quartzo-feldspathic gneisses of the Oaxacan Complex. The pyroxenite, as well as the pegmatite body, do not show any sign of deformation. The pegmatite is composed of diopside megacrysts (up to 40 cm long) in contact with scapolite, or symplectitic intergrowth of these two minerals, phlogopite and a calcite core. It also presents dispersed megacrysts (up to 10 cm) of zircon, titanite and apatite; these minerals are mainly located in the contact between scapolite, diopside crystals and the calcite core. The crystals of zircon and titanite show petrographic evidence of crystallizing at equilibrium with diopside, which means that they have crystallized during the early stage of the pegmatite formation. During the field work no presence was found of the classical quartz core or any other manifestation of quartz in this pegmatite body. Dated zircon fragments were taken from euhedral megacrysts of ~2 cm and smaller in length, elongated, prismatic with bipyramidal terminations and with well-defined facets, and colored pink to purple. The obtained U-Pb ages of 20 spots vary from 955 to 1005 Ma, with a mean age of 981.4 ± 7.1 Ma (MSWD = 2.2) (Figure 2d). The analyzed zircons display relatively uniform low Y (avg = 263) and moderate Hf (avg = 7045) concentrations. Th/U ratios range between 0.38 and 0.68. These zircons show also similar REE patterns (Figure 2e), steeply increasing from La to Lu (Lu_N/La_N avg = 6556), a strong positive Ce/Ce^* (avg = 43.3) and a very slight negative Eu/Eu^* anomalies (avg = 0.45). The HREE enrichment expressed by the Lu_N/Gd_N value averages 37.6 and the average Sm_N/La_N value is 47.8.

Pegmatite sample AYQ25-7

This sample was taken from one dike belonging to a group of 30 – 60 cm wide pegmatite dikes cutting the host biotite-quartzo-feldspathic gneiss. It consists of an intergrowth of quartz and highly epidotized microcline in the central zone and a border zone composed by epidotized feldspars, biotite, altered ilmenite with secondary titanite, and abundant zircon crystals. The latter are fractured euhedral megacrysts measuring up to 2 mm in length, with bipyramidal terminations and well-defined facets, pink to purple colored. The obtained U-Pb ages of 25 spots vary from 931 to 1000 Ma, with a mean age of 963 ± 7 Ma (MSWD = 2.5) (Figure 2f). The analyzed zircons display low Y (avg = 268), as well as uniform and moderate Hf (avg = 9425) concentrations, and high Th/U ratios of 0.55 – 0.89. The REE patterns are also homogeneous, smoothly increasing from La to Lu (Lu_N/La_N avg = 1504), with strong positive Ce/Ce^* (avg = 35.3) and negative Eu/Eu^* (avg = 0.25) anomalies (Figure 2g). The HREE enrichment is characterized by Lu_N/Gd_N avg = 14.1; the average value of Sm_N/La_N is 35.8.

Pegmatite sample 176-1

This sample is part of a moderately deformed 0.5 – 1 m wide pegmatite dike that intrudes the amphibolite gneiss host rock. The pegmatite dike does not show much zonation from borders to center. It is mainly composed of altered amphibole megacrysts (>15 cm), quartz, K-feldspar, mesoperthite, magnetite-titanomagnetite, and

accessory zircons. The zircon crystals are always in association with hornblende, and their morphological character gives evidence that they crystallized during the early stage of the pegmatite formation. All analyzed zircon crystals are smaller than 200 μm in length, euhedral, prismatic elongated with bipyramidal terminations, and slightly pink-colored. We analyzed 2 spots from small cores and 23 spots from rims (Figure 2k). The obtained U-Pb ages of the cores are concordant at 1156 ± 24 and 1134 ± 25 Ma and the rim ages vary from 953 to 993 Ma with a mean age of 977 ± 4.6 Ma (MSWD = 0.89) (Figure 2i). The Y concentrations vary from 162 to 993 ppm (avg = 416) whereas Hf ranges from 9200 to 13984 ppm (avg = 11451). Th/U ratios are uniformly high (0.29 – 0.71), with the exception of one spot (Th/U = 0.08) located in the core. Other geochemical signatures of these zircons are homogeneous REE patterns, steeply increasing from La to Lu (Lu_N/La_N avg = 4567), with well-defined positive Ce/Ce^* (avg = 10.4) and negative Eu/Eu^* (avg = 0.14) anomalies (Figure 2j). The cores have REE patterns slightly different from the rims, and show the strongest ($\text{Eu}/\text{Eu}^* = 0.03$), as well as the weakest ($\text{Eu}/\text{Eu}^* = 0.22$) Eu anomaly. HREE enrichment is characterized by Lu_N/Gd_N avg = 13.1 and the average value of Sm_N/La_N is 126.1.

Pegmatite sample 183-2

This sample was taken from a 0.5 – 1 m sized pegmatite dike cutting the host rock (quartzo-feldspathic gneiss). It is composed of large (1 – 2 cm) crystals of ilmenite with secondary titanite, calcite megacrysts (up to 5 cm), quartz, altered calcic feldspars and abundant crystals of zircon. Zircon crystals are euhedral and less than 200 μm in length, prismatic elongated with bipyramidal terminations, pink-colored and always show spatial relation with Fe-oxides. The obtained ages of 32 spots vary from 938 to 995 Ma, with a mean age of 969.8 ± 4.6 Ma (MSWD = 1.3) (Figures 2l and 2n). Hf concentrations in the zircons belonging to this sample range from 9989 to 13664 ppm (avg = 11693), whereas Y ranges from 208 to 1043 ppm (avg = 508), and Th/U ratios are uniformly high between 0.46 and 0.95. These zircons have homogeneous REE patterns, gradually rising from La to Lu (Lu_N/La_N avg = 2522), with well-defined positive Ce/Ce^* (avg = 25.9) and negative Eu/Eu^* (avg = 0.21) anomalies (Figure 2m). The HREE enrichment is characterized by Lu_N/Gd_N avg = 12.2 and the average value of Sm_N/La_N is 76.1.

Pegmatite-migmatite (leucosome) sample 213-1

A series of pegmatite-migmatite (leucosome) lenses (1 – 5 m wide and some meters long) are located within a mafic host rock (amphibolite gneiss). According to Mehnert (1968) and London and Černý (2008), this group of pegmatite bodies could be named pegmatite-migmatite: the lenses are concordant with the foliation of the host rock, the limits between pegmatite bodies and the host rock are not well defined, and there is no internal zonation of the pegmatite body. The series of pegmatite leucosome lenses consist of megacrysts (up to 5 cm and more) of chloritized amphiboles, sericitized andesine-labradorite, perthitic microcline, opaque Fe-minerals (magnetite-titanomagnetite-ilmenite), apatite, abundant zircon, and small amounts of quartz (<5%). The analyzed zircon crystals have irregular subhedral form, are up to 200 μm in length, prismatic, elongated with bipyramidal terminations, pink-colored and are in association with hornblende and Fe-oxides. The obtained U-Pb ages of 27 spots vary from 927 to 1035 Ma, with a mean age of 980.1 ± 4.7 Ma (MSWD = 0.98) (Figures 2o and 2q). The zircons separated from this sample have uniform and moderate Hf concentrations (9521 – 12439 ppm; avg = 11020) and relatively low concentrations of Y (204 – 632 ppm; avg = 362). Th/U ratios are uniformly high between 0.47 and 0.86. They also have homogeneous REE patterns, steeply increasing from La to Lu (Lu_N/La_N avg = 4272),

Table 2. Concentrations of trace elements in ppm from studied zircons.

	Y	La	Ce	Pr	Nd	Sm	Eu	Gd	Tb	Dy	Ho	Er	Yb	Lu	Hf
La Ofelia															
<i>rims</i>															
Zircon_01_LaOfelia_008	496	0.18	11.23	0.21	4.31	3.19	0.57	12.36	3.95	44.99	16.91	71.09	119.21	21.47	12212
Zircon_06_014	618	0.13	8.23	0.17	3.97	3.81	0.48	12.68	4.28	53.04	20.78	97.73	209.87	41.46	13562
Zircon_07_015	552	0.12	9.42	0.20	3.99	3.20	0.69	11.63	4.02	48.96	19.25	92.26	196.23	37.91	13050
Zircon_13_022	600	0.14	14.44	0.22	3.14	4.54	0.79	17.67	5.56	59.14	20.94	85.24	131.50	23.60	13370
Zircon_14_023	658	0.13	11.98	0.26	3.15	2.58	0.48	11.38	4.22	54.02	21.89	109.18	233.94	46.87	15091
Zircon_15_024	598	0.22	10.79	0.26	3.73	3.35	0.69	13.71	4.68	56.15	21.13	91.53	163.93	30.19	12691
Zircon_16_026	631	0.09	11.18	0.16	2.56	2.17	0.34	10.60	4.00	52.60	22.39	110.81	247.45	47.68	12501
Zircon_17_027	712	0.12	9.68	0.23	3.58	3.28	0.90	14.12	5.04	62.91	25.34	120.79	262.36	53.05	15957
Zircon_23_034	665	0.11	10.77	0.23	3.59	3.88	0.48	13.26	4.54	56.18	23.27	112.40	239.15	48.73	15111
Zircon_27_039	603	0.13	10.90	0.15	3.31	3.44	0.72	12.79	4.56	57.55	21.97	101.13	199.73	38.19	13273
Zircon_29_041	652	0.12	11.33	0.19	2.69	2.81	0.41	12.41	4.48	55.33	22.83	108.51	234.50	48.10	14685
<i>cores</i>															
Zircon_02_009	647	0.16	11.22	0.27	3.58	3.07	0.45	12.79	4.44	56.33	22.01	105.15	217.64	41.70	11680
Zircon_03_010	2194	0.18	42.09	0.32	5.47	9.83	1.24	52.93	17.79	207.34	77.41	337.98	629.39	114.87	12137
Zircon_04_011	590	0.17	13.02	0.22	3.82	2.69	0.34	9.11	3.57	46.09	20.10	104.57	249.67	52.03	12627
Zircon_05_012	614	0.13	13.94	0.20	3.72	4.00	0.53	12.26	4.29	54.89	20.79	99.17	203.08	39.93	13023
Zircon_08_016	765	0.15	16.65	0.21	4.22	3.43	0.58	14.92	5.51	69.03	26.98	130.73	272.19	52.43	12152
Zircon_09_017	663	0.16	13.63	0.22	3.83	2.94	0.53	13.55	4.93	59.05	23.24	111.04	224.41	43.18	12195
Zircon_10_018	751	0.11	17.12	0.19	3.64	3.47	0.56	16.67	5.50	67.93	26.50	123.52	254.56	49.11	12867
Zircon_11_020	737	0.15	19.11	0.21	3.13	3.53	0.77	15.71	5.43	66.12	25.45	120.13	238.55	45.84	10925
Zircon_12_021	1617	0.15	47.94	0.27	4.14	6.27	0.76	33.20	11.43	143.06	56.67	269.41	545.48	103.36	12516
Zircon_18_028	674	0.12	13.42	0.14	3.23	2.89	0.51	13.27	4.47	57.69	23.72	114.94	242.28	49.40	13420
Zircon_19_029	975	0.18	22.07	0.21	3.20	2.88	0.53	14.62	5.48	76.53	33.42	170.80	401.59	81.86	14517
Zircon_20_030	857	0.10	26.51	0.17	4.21	3.08	0.33	16.18	5.51	74.63	30.48	150.31	326.71	63.40	13776
Zircon_24_035	1109	0.07	27.01	0.20	3.53	4.47	0.61	19.25	7.10	92.71	39.63	193.65	411.11	82.78	12003
Zircon_25_036	653	0.14	13.73	0.17	3.02	2.97	0.56	13.98	4.75	60.51	23.82	113.02	235.35	45.70	11485
Zircon_26_038	1284	0.09	29.91	0.19	3.06	4.22	0.55	22.21	8.27	112.04	46.39	225.95	476.76	92.16	10023
Zircon_28_040	1455	0.08	46.73	0.18	4.78	5.85	0.65	27.23	10.19	131.00	53.45	255.52	533.08	102.80	14207
Zircon_30_LaOfelia_042	737	0.19	17.74	0.22	3.99	3.58	0.42	15.03	5.62	67.92	27.00	131.28	261.41	51.53	16395
La Panchita															
Zircon_21_PANchita2	224	0.03	6.66	0.08	0.97	1.11	0.42	3.98	1.34	15.72	6.54	32.60	78.20	15.94	5120
Zircon_22	264	0.23	9.93	0.17	1.87	1.41	0.61	5.47	1.60	20.17	7.57	38.00	88.90	18.75	5800
Zircon_23	244	n/d	8.01	0.07	0.90	1.00	0.47	4.79	1.61	17.70	7.32	37.30	90.00	18.34	5770
Zircon_24	257	0.00	8.08	0.05	0.92	0.98	0.47	4.99	1.64	18.46	7.70	37.70	93.20	18.67	5770
Zircon_25	274	0.02	8.84	0.07	1.14	1.37	0.49	5.01	1.85	20.30	8.58	41.10	100.70	20.30	6320
Zircon_26	234	n/d	7.27	0.05	0.77	0.91	0.39	4.58	1.47	17.00	6.91	34.80	85.20	17.02	5270
Zircon_27	273	0.20	8.89	0.11	1.27	1.62	0.51	5.79	1.81	19.90	8.22	40.70	98.60	19.93	6140
Zircon_28	262	n/d	8.23	0.04	0.96	1.26	0.44	5.76	1.62	19.60	8.09	40.20	95.20	19.84	6160
Zircon_29	119	0.10	6.55	0.05	0.50	0.46	0.15	1.77	0.71	8.05	3.31	17.70	46.90	10.17	5880
Zircon_30_PANchita2	279	0.02	8.75	0.08	1.09	1.54	0.39	5.57	1.67	21.00	8.39	42.50	105.30	20.97	6510
Zircon_31_PANchita3	211	0.02	4.60	0.02	0.36	0.55	0.29	3.42	1.13	14.66	6.43	33.50	85.10	18.23	6490
Zircon_32	260	n/d	5.52	0.03	0.70	0.71	0.26	4.79	1.39	18.80	7.72	40.80	105.80	22.23	7970
Zircon_33	285	n/d	6.00	0.04	0.56	0.89	0.37	3.79	1.42	19.00	8.19	42.00	113.80	23.66	7920
Zircon_34	235	0.01	5.48	0.04	0.63	0.78	0.22	3.66	1.15	16.50	7.21	35.80	95.00	20.24	7410
Zircon_35	304	n/d	6.16	0.03	0.54	0.97	0.34	4.62	1.62	20.10	8.97	47.70	122.90	26.38	8600
Zircon_36	233	n/d	4.71	0.03	0.35	0.55	0.22	3.67	1.14	16.20	7.09	36.60	97.20	20.53	6600
Zircon_37	296	n/d	6.12	0.03	0.45	0.75	0.25	4.82	1.53	20.80	8.59	46.40	126.30	26.40	8990
Zircon_38	276	0.00	5.92	0.02	0.53	0.69	0.30	3.51	1.52	19.20	8.25	42.50	113.90	24.00	8220
Zircon_39	323	0.02	6.70	0.04	0.65	0.87	0.39	5.33	1.68	20.50	9.65	51.20	131.60	28.32	9280
Zircon_40_PANchita3	401	n/d	7.58	0.04	0.69	0.80	0.45	6.01	2.16	27.00	11.67	60.90	160.60	34.60	10690
AYQ25-7															
Zircon_02_009	273	0.04	12.64	0.08	1.32	2.05	0.37	8.51	2.48	25.92	9.12	38.32	78.90	14.60	10345
Zircon_03_010	525	0.02	19.49	0.18	3.17	5.34	0.84	21.29	5.71	55.37	17.76	68.51	120.33	21.30	9541

continues

Table 2 (cont.). Concentrations of trace elements in ppm from studied zircons.

	Y	La	Ce	Pr	Nd	Sm	Eu	Gd	Tb	Dy	Ho	Er	Yb	Lu	Hf
AYQ25-7 (cont.)															
Zircon_04_011	230	0.02	14.91	0.06	1.02	1.30	0.22	5.39	1.66	19.59	7.37	33.70	80.06	16.10	9720
Zircon_05_012	231	0.26	13.85	0.22	1.69	1.90	0.38	7.71	2.08	21.78	7.17	30.39	57.72	10.47	8320
Zircon_08_016	177	0.10	10.94	0.04	0.95	1.32	0.23	5.05	1.59	18.03	5.86	24.83	52.05	10.02	9890
Zircon_12_021	335	0.18	15.58	0.16	2.10	1.99	0.37	8.05	2.41	27.08	10.29	47.47	107.79	20.82	9273
Zircon_13_022	164	0.02	9.05	0.06	0.91	0.98	0.21	4.74	1.35	14.60	5.35	23.43	48.37	9.06	9007
Zircon_14_023	221	0.01	10.16	0.08	1.15	1.54	0.29	6.74	1.99	21.23	7.41	31.44	65.23	12.26	9223
Zircon_15_024	258	0.33	10.65	0.24	2.45	2.58	0.49	8.23	2.34	24.20	8.35	35.32	69.49	13.29	9569
Zircon_16_026	235	0.30	11.16	0.16	1.59	1.54	0.26	6.90	2.02	23.06	7.73	33.32	72.97	13.24	10138
Zircon_17_027	663	0.44	15.49	0.28	2.68	3.75	0.74	17.90	5.70	61.03	21.77	92.18	182.26	33.78	10483
Zircon_18_028	302	0.10	19.69	0.13	1.50	2.37	0.42	10.03	2.91	30.22	10.00	41.71	78.51	14.13	9625
Zircon_20_030	158	0.08	12.09	0.07	1.72	1.26	0.21	5.04	1.47	15.87	5.11	21.77	44.48	8.23	10221
Zircon_21_032	194	0.02	11.66	0.08	1.18	1.70	0.23	6.50	1.85	18.78	6.64	26.91	53.25	9.82	8220
Zircon_22_033	492	0.01	13.82	0.05	1.82	2.66	0.52	14.34	4.34	46.74	16.48	66.95	122.76	22.59	9433
Zircon_23_034	169	0.06	13.07	0.06	0.72	0.77	0.15	3.69	1.24	13.53	5.37	25.41	57.38	11.42	8900
Zircon_24_035	177	0.01	11.89	0.05	1.09	1.55	0.18	5.71	1.62	16.83	5.85	24.71	48.73	9.17	9409
Zircon_25_036	293	0.02	16.62	0.07	1.03	1.42	0.24	6.30	2.08	23.53	9.22	42.97	96.85	19.28	9352
Zircon_26_038	205	0.02	12.16	0.05	0.67	1.13	0.20	4.10	1.46	16.97	6.53	30.38	68.93	13.72	9795
Zircon_27_039	203	0.01	11.18	0.05	0.78	1.01	0.18	4.40	1.31	16.56	6.28	29.90	68.83	13.39	8806
Zircon_28_040	193	0.00	11.88	0.06	0.76	0.99	0.19	4.14	1.41	15.89	5.90	27.66	63.99	12.29	8009
Zircon_29_041	284	0.03	14.08	0.06	1.06	1.79	0.31	6.27	1.96	23.80	8.84	40.42	92.45	18.40	9216
Zircon_30_042	296	0.15	14.79	0.14	1.43	1.79	0.31	7.02	2.09	24.66	9.37	43.80	97.07	19.02	9127
Zircon_31_044	220	0.01	14.41	0.06	0.90	1.08	0.21	4.75	1.50	17.94	7.07	32.13	74.68	14.93	9900
Zircon_32_045	206	0.26	16.87	0.16	1.57	1.27	0.25	6.41	1.68	18.30	6.68	29.25	63.48	12.63	10100
176-1															
<i>rims</i>															
Zircon_96_D_122	346	0.03	8.04	0.12	1.59	2.78	0.32	11.39	3.26	35.46	12.38	52.05	98.92	19.18	11851
Zircon_97_123	302	0.12	6.73	0.13	1.98	2.56	0.31	9.16	2.81	29.64	10.61	46.49	90.57	17.50	10130
Zircon_99_125	559	0.06	8.12	0.31	5.29	7.34	0.70	21.97	6.23	62.37	19.88	81.01	145.25	27.59	10941
Zircon_100_126	236	0.03	5.68	0.08	1.59	1.98	0.19	8.65	2.20	23.32	7.76	33.21	61.49	11.55	10426
Zircon_101_128	316	0.14	3.75	0.10	1.67	2.12	0.25	8.36	2.63	29.90	10.82	52.48	124.09	27.17	12047
Zircon_102_129	317	0.03	6.95	0.20	1.89	2.29	0.28	9.50	2.78	29.98	11.11	48.96	103.21	20.91	11828
Zircon_104_131	211	0.06	3.93	0.11	1.65	1.93	0.15	6.66	1.97	20.69	7.39	32.74	68.07	14.12	11330
Zircon_105_132	351	0.04	3.37	0.09	1.61	1.68	0.22	8.90	2.75	32.64	12.17	56.44	126.29	26.69	10188
Zircon_106_134	209	0.01	5.58	0.08	1.60	2.04	0.14	7.32	1.86	21.42	7.22	32.13	62.84	12.82	11723
Zircon_107_135	406	0.07	4.15	0.16	1.68	2.45	0.22	9.99	3.25	37.84	14.53	69.14	153.70	32.24	12334
Zircon_108_136	812	0.04	8.46	0.58	9.09	11.80	1.15	37.80	9.52	91.58	29.43	113.66	201.02	37.00	10699
Zircon_109_137	234	0.07	5.92	0.11	1.69	2.21	0.18	7.03	2.21	22.97	8.28	35.70	72.14	14.11	12376
Zircon_110_138	302	n/d	6.25	0.15	2.35	2.31	0.30	9.45	2.82	29.30	10.48	45.21	87.89	17.11	11263
Zircon_111_140	716	0.04	8.77	0.50	9.08	11.43	1.06	32.64	8.38	81.86	25.77	102.34	176.72	33.14	11276
Zircon_112_141	205	0.05	5.29	0.11	1.76	1.73	0.13	6.62	1.88	19.54	7.16	30.83	62.10	12.28	12228
Zircon_114_143	342	0.08	7.73	0.11	1.97	2.64	0.39	10.45	3.34	35.41	12.10	52.36	97.97	18.65	10863
Zircon_115_144	372	0.04	5.11	0.20	4.17	4.52	0.46	15.37	4.04	41.09	13.76	55.51	102.50	20.05	10153
Zircon_116_146	162	0.06	4.78	0.11	1.82	1.65	0.22	5.77	1.46	15.17	5.85	27.38	59.43	12.12	13984
Zircon_117_147	256	0.03	5.04	0.13	1.51	1.88	0.18	6.84	2.03	23.69	8.65	39.48	86.81	17.08	12489
Zircon_118_148	645	0.06	8.95	0.30	5.11	7.34	0.69	26.39	6.97	71.63	23.13	94.95	166.69	32.14	12417
Zircon_119_149	710	0.06	7.34	0.29	5.11	7.85	0.94	31.53	8.28	81.30	26.27	105.79	181.64	34.14	11223
Zircon_120_150	368	0.03	5.50	0.14	2.43	2.43	0.29	10.79	3.35	37.76	13.07	57.68	107.52	20.70	10681
Zircon_123_D_154	568	0.03	4.97	0.19	2.15	3.20	0.37	15.92	4.95	55.29	20.27	89.80	191.22	38.73	11515
<i>cores</i>															
Zircon_98_124	469	0.02	3.56	0.13	1.45	2.23	0.09	13.62	4.55	49.05	16.74	74.57	141.82	27.28	13104
Zircon_103_130	993	0.09	6.70	0.29	5.75	8.74	1.55	36.17	10.59	110.15	37.34	153.43	278.24	52.74	9200
183-2															
Zircon_01_A_008	265	0.14	21.82	0.19	3.07	2.88	0.51	7.71	2.37	25.48	8.78	38.37	79.06	15.45	12327
Zircon_02_009	766	0.10	23.65	0.45	7.35	8.63	1.32	31.00	8.51	83.42	26.43	105.67	189.36	35.69	10550
Zircon_03_010	337	0.01	24.45	0.23	2.94	2.41	0.46	9.85	2.75	31.60	11.21	49.32	99.98	19.60	12190

continues

Table 2 (cont.). Concentrations of trace elements in ppm from studied zircons.

	Y	La	Ce	Pr	Nd	Sm	Eu	Gd	Tb	Dy	Ho	Er	Yb	Lu	Hf
183-2 (cont.)															
Zircon_04_011	347	0.06	24.52	0.20	2.76	2.74	0.45	10.82	3.01	32.67	11.52	49.43	100.63	20.07	11011
Zircon_05_012	208	0.07	14.73	0.16	2.43	1.96	0.31	6.28	1.70	19.55	6.88	30.00	61.76	12.04	10640
Zircon_07_015	410	0.11	24.59	0.24	3.34	2.45	0.56	11.24	3.32	37.17	13.61	60.34	120.70	23.51	12097
Zircon_08_016	397	0.15	26.02	0.20	3.29	3.25	0.47	12.24	3.53	37.74	13.27	58.50	114.48	23.01	12040
Zircon_09_017	599	0.10	23.91	0.27	4.50	5.37	0.89	20.15	5.86	61.25	20.84	86.97	160.64	30.87	11538
Zircon_10_018	259	0.17	13.19	0.15	2.58	2.13	0.36	7.88	2.34	24.71	8.62	38.61	77.83	15.64	10960
Zircon_11_020	402	0.07	30.37	0.23	3.85	3.54	0.45	11.72	3.52	39.12	13.41	59.80	121.82	24.64	13643
Zircon_12_021	546	0.07	20.37	0.18	3.01	3.88	0.66	17.21	5.04	54.14	19.20	80.18	148.20	28.21	10726
Zircon_13_022	510	0.13	27.53	0.20	3.84	4.12	0.61	16.30	4.48	50.97	17.81	74.69	142.07	27.45	11339
Zircon_14_023	282	0.17	19.46	0.17	2.63	2.30	0.30	7.71	2.75	26.69	9.72	41.65	85.21	17.05	13298
Zircon_15_024	829	0.03	26.63	0.19	3.05	4.64	0.75	24.63	7.44	82.79	29.02	120.13	220.82	41.44	11856
Zircon_16_026	859	0.16	27.26	0.29	4.10	5.44	0.92	27.06	8.09	86.56	29.82	124.28	225.91	42.40	12008
Zircon_17_027	389	0.14	23.10	0.21	3.29	3.22	0.39	12.52	3.59	39.88	13.44	59.92	119.97	23.55	13665
Zircon_18_028	890	0.13	26.30	0.74	11.20	12.79	1.80	40.11	10.32	100.48	33.04	130.85	225.82	42.69	9989
Zircon_19_029	447	0.03	20.56	0.16	3.08	3.96	0.59	14.89	4.33	46.70	16.13	67.24	131.25	24.72	10215
Zircon_20_030	261	0.10	20.67	0.18	2.64	2.37	0.33	7.88	2.49	26.51	9.12	40.55	81.70	16.25	12536
Zircon_21_032	275	0.14	20.03	0.24	2.64	2.36	0.33	8.63	2.63	28.31	9.80	42.54	86.06	16.92	13552
Zircon_22_033	558	0.10	22.22	0.23	4.51	5.82	1.14	22.78	6.13	60.98	20.74	84.30	147.71	28.51	11176
Zircon_23_034	657	0.11	22.26	0.53	7.80	9.03	1.23	27.06	7.52	72.99	23.76	99.34	173.85	32.94	10051
Zircon_24_035	583	0.06	28.10	0.24	4.27	5.04	0.86	19.91	5.77	59.22	20.40	83.82	153.91	29.03	11268
Zircon_25_036	414	0.10	18.27	0.18	3.26	3.63	0.60	14.11	3.98	43.23	14.60	60.23	113.71	22.30	11620
Zircon_26_038	618	0.09	22.25	0.31	4.56	6.48	0.86	23.55	6.46	65.89	22.31	90.96	166.01	31.75	11107
Zircon_27_039	480	0.07	30.60	0.29	3.38	3.43	0.64	15.82	4.66	48.88	16.77	71.96	137.54	26.66	12840
Zircon_28_040	458	0.06	23.29	0.19	2.68	3.03	0.48	13.91	4.29	44.48	15.90	67.88	131.43	25.67	11302
Zircon_29_041	966	0.17	26.89	1.06	13.17	15.12	2.15	45.22	11.53	109.95	34.82	133.69	230.58	42.29	11178
Zircon_30_042	330	0.06	25.95	0.14	2.19	2.69	0.38	9.13	2.86	30.74	10.93	47.93	97.18	18.92	11617
Zircon_31_044	1043	0.14	23.37	0.78	10.75	13.51	2.18	43.89	12.05	116.00	37.57	149.15	258.54	48.60	11401
Zircon_32_045	492	0.15	21.33	0.25	3.03	4.19	0.59	15.98	4.65	49.46	17.28	73.12	142.11	27.80	12044
Zircon_33_A_046	389	0.10	19.33	0.16	3.17	3.24	0.41	12.32	3.56	39.70	13.80	57.82	110.85	22.05	12384
213-1															
Zircon_64_C_083	293	0.11	16.26	0.15	1.74	2.13	0.44	9.49	2.62	29.30	10.28	45.15	91.63	18.17	11584
Zircon_65_084	488	0.05	17.01	0.18	3.11	3.50	0.58	15.58	4.48	48.51	16.92	74.01	139.43	27.86	12439
Zircon_66_086	406	0.04	14.37	0.15	2.38	2.61	0.51	12.17	3.63	39.30	14.17	61.80	117.54	23.52	11005
Zircon_67_087	528	0.09	15.65	0.17	3.34	4.94	0.81	20.05	5.34	56.05	19.04	77.01	140.68	26.85	10573
Zircon_68_088	229	0.07	11.16	0.13	1.96	2.08	0.28	6.57	2.01	22.57	8.11	35.07	70.91	14.24	10917
Zircon_69_089	632	0.04	18.42	0.23	3.90	6.53	0.94	22.75	6.31	67.18	22.76	93.29	170.28	32.89	11277
Zircon_71_092	228	0.04	14.48	0.13	1.56	1.53	0.24	7.09	1.99	22.08	7.96	35.98	72.89	14.09	11375
Zircon_72_093	585	0.06	17.33	0.23	3.02	4.85	0.96	20.96	5.79	60.72	20.30	84.86	156.36	29.08	10385
Zircon_73_094	474	0.03	15.55	0.17	2.49	3.06	0.50	13.48	4.26	46.28	16.82	71.94	136.85	26.41	11140
Zircon_74_095	450	0.05	15.20	0.15	2.30	2.98	0.53	12.96	4.04	43.43	16.03	69.09	129.30	25.62	10823
Zircon_75_096	239	0.02	12.24	0.18	2.11	2.17	0.32	6.57	2.17	23.50	8.45	36.31	75.27	14.87	11916
Zircon_76_098	204	0.05	10.25	0.13	1.63	2.05	0.23	6.22	1.81	20.56	7.47	32.65	66.30	13.15	11122
Zircon_78_100	282	0.07	14.67	0.15	2.02	2.49	0.41	8.70	2.76	29.03	10.13	43.70	87.02	17.57	10506
Zircon_79_101	290	0.04	12.83	0.11	1.82	2.07	0.38	9.40	2.51	28.43	10.36	45.93	90.47	18.09	11242
Zircon_80_102	268	n/d	15.07	0.15	2.32	2.12	0.34	8.68	2.38	26.52	9.43	41.45	83.20	16.59	11489
Zircon_82_105	507	0.06	15.14	0.18	2.81	4.36	0.63	15.85	4.68	52.16	18.31	77.62	142.86	27.66	10320
Zircon_83_106	469	0.04	15.95	0.20	2.28	3.13	0.60	13.08	4.03	45.18	16.62	71.95	137.05	26.92	11473
Zircon_84_107	223	0.01	10.66	0.15	1.61	1.57	0.28	6.63	2.02	22.23	7.93	34.21	69.13	13.50	10828
Zircon_85_108	429	0.04	16.10	0.14	2.47	3.06	0.50	11.60	3.65	41.84	15.16	65.69	124.35	24.18	10288
Zircon_87_111	362	0.00	16.20	0.09	1.47	1.54	0.44	7.63	2.63	32.73	12.83	61.37	139.29	29.35	12045
Zircon_88_112	284	0.09	11.45	0.14	1.77	1.95	0.51	8.60	2.57	28.43	10.08	43.56	86.21	17.44	10286
Zircon_90_114	267	0.07	13.19	0.13	1.66	1.38	0.40	6.10	1.85	23.22	9.10	44.44	106.61	23.63	11084
Zircon_91_116	322	0.08	15.53	0.11	2.05	2.72	0.44	9.36	2.79	31.93	11.32	51.57	105.90	21.08	11048
Zircon_92_117	215	0.05	15.72	0.13	1.90	1.64	0.26	6.83	1.91	21.01	7.40	33.69	66.54	13.12	12111
Zircon_93_118	261	0.01	15.48	0.10	1.83	2.11	0.29	8.30	2.47	25.69	9.14	40.08	78.55	15.55	10783

continues

Table 2 (cont.). Concentrations of trace elements in ppm from studied zircons.

	Y	La	Ce	Pr	Nd	Sm	Eu	Gd	Tb	Dy	Ho	Er	Yb	Lu	Hf
213-1 (cont.)															
Zircon_94_119	529	0.04	14.64	0.10	2.38	4.16	0.75	16.22	5.20	54.84	18.80	80.70	145.82	28.32	9972
Zircon_95_C_120	312	0.04	14.89	0.13	1.74	2.04	0.42	9.63	2.97	31.88	10.87	47.90	94.39	18.61	9522
OC22-4AB															
<i>rims</i>															
Zircon_03_010	514	0.05	4.24	0.10	1.24	1.58	0.05	7.88	2.85	38.58	15.27	77.92	198.56	38.38	11066
Zircon_05_012	1137	0.09	2.46	0.10	1.17	2.07	0.41	15.05	6.90	92.70	37.19	172.95	383.93	70.69	12442
Zircon_10_018	1692	0.03	1.80	0.05	1.15	2.46	0.08	21.47	10.27	138.70	54.81	258.11	558.81	102.19	11790
Zircon_11_020	1000	0.04	2.41	0.12	1.85	3.05	0.05	17.50	6.85	86.63	33.62	156.70	356.14	66.74	20051
Zircon_23_034	1316	0.19	2.06	0.10	1.20	2.50	0.08	18.93	8.65	114.20	43.29	198.28	427.62	77.14	7090
Zircon_30_042	648	0.10	2.15	0.10	1.23	1.98	1.37	11.00	4.20	53.31	20.74	97.32	217.43	41.81	10742
<i>cores</i>															
Zircon_01_OC22-4a_008	2007	0.12	3.26	0.16	2.46	3.94	0.70	27.73	12.67	164.47	64.92	299.32	657.81	121.88	15183
Zircon_02_009	1247	0.04	1.80	0.07	1.06	1.76	0.05	11.81	5.71	84.45	39.11	224.56	731.91	147.55	13225
Zircon_04_011	2194	0.00	4.43	0.09	1.65	4.65	0.18	36.00	15.64	197.63	73.13	319.71	630.52	112.07	12473
Zircon_07_015	1974	0.03	2.04	0.09	1.52	4.23	0.13	28.68	12.90	169.52	65.35	297.49	638.21	115.85	10574
Zircon_08_016	1366	0.05	2.94	0.13	1.82	2.94	0.76	20.49	8.96	113.52	44.16	205.89	457.00	84.43	14806
Zircon_09_017	1066	0.01	2.54	0.05	1.00	1.92	0.05	14.44	6.52	88.46	34.88	162.33	357.03	65.86	12428
Zircon_12_021	1311	0.03	2.06	0.06	1.09	2.49	0.09	17.02	8.22	108.42	43.02	204.66	466.18	85.67	14146
Zircon_13_022	1267	0.00	2.67	0.10	1.34	2.28	0.52	18.77	8.22	108.06	41.92	192.30	435.89	80.63	13100
Zircon_14_023	893	0.06	2.58	0.10	1.25	1.76	1.25	11.56	5.46	73.88	28.62	137.83	316.45	57.77	11654
Zircon_15_024	1232	0.02	1.85	0.06	1.00	1.86	0.19	15.93	7.32	100.10	39.84	192.56	440.83	82.28	12275
Zircon_17_027	2017	0.03	2.73	0.08	1.08	2.75	0.06	22.36	11.05	154.59	64.52	323.89	802.20	153.48	15088
Zircon_19_029	2155	0.04	2.70	0.14	2.29	6.58	0.16	39.74	16.07	195.38	71.65	317.15	660.30	118.09	11770
Zircon_20_030	1518	0.02	2.15	0.06	1.18	3.21	0.10	21.85	9.81	128.93	49.49	227.65	487.95	89.78	11638
Zircon_21_032	2061	0.08	4.38	0.15	2.25	5.06	0.41	32.38	14.20	180.28	68.17	315.20	706.75	129.93	13341
Zircon_22_033	2980	0.28	4.11	0.27	3.07	6.31	0.71	46.24	19.86	257.11	99.18	446.38	968.44	176.65	12317
Zircon_24_035	2288	0.21	2.75	0.13	2.09	4.67	0.13	32.67	14.81	196.74	76.68	351.02	776.48	144.35	12766
Zircon_25_036	1371	0.23	8.36	0.29	2.88	3.61	2.17	21.17	8.96	117.39	45.60	208.82	463.36	85.95	12958
Zircon_26_038	3202	0.02	2.83	0.15	2.01	5.59	0.27	45.71	20.59	274.16	105.86	488.70	1059.54	195.27	16074
Zircon_27_039	909	0.05	1.76	0.09	1.27	2.56	0.09	14.37	5.86	77.34	30.18	141.91	331.00	62.49	12629
Zircon_28_OC22-4B_040	1499	0.19	4.41	0.21	1.69	3.34	0.59	21.70	9.71	125.61	47.80	224.18	479.89	91.40	12018
Zircon_29_041	1867	0.04	1.89	0.05	1.08	2.68	0.09	24.96	10.83	150.31	58.83	277.26	604.64	113.81	12889
Zircon_31_044	2392	0.44	5.52	0.47	3.38	5.83	0.95	34.91	15.25	204.35	76.98	357.42	771.84	147.77	12549
Zircon_32_045	1691	0.23	5.58	0.28	2.48	3.37	2.23	22.98	10.15	139.09	54.25	256.51	557.02	105.22	11213
Zircon_33_046	3452	1.18	6.57	0.51	5.89	7.75	2.08	51.64	21.69	292.26	111.50	510.26	1103.70	213.13	15321
Zircon_35_048	2847	0.04	3.89	0.23	4.46	9.74	0.20	59.25	23.19	275.43	96.38	412.96	801.99	144.81	12863
Zircon_36_050	3166	0.03	3.88	0.16	3.29	6.97	0.15	54.02	22.76	282.54	104.12	460.29	954.76	177.05	16829
Zircon_37_051	536	0.01	1.61	0.04	0.55	0.61	0.05	6.67	3.11	41.55	17.25	81.64	190.08	37.06	13386
Zircon_38_052	2231	0.89	6.02	0.56	3.90	5.53	1.71	35.14	14.61	194.45	72.92	338.34	727.79	138.65	12231
Zircon_40_054	2279	0.34	5.88	0.39	4.02	8.24	1.27	47.69	18.23	218.49	75.43	323.36	620.84	113.94	10724
Zircon_41_056	3372	0.06	4.57	0.31	5.33	12.12	0.30	72.16	26.80	319.26	112.64	478.54	915.55	167.30	15887
Zircon_42_057	2492	0.08	2.92	0.18	2.05	4.39	0.82	35.63	15.62	210.58	81.46	372.76	794.69	148.25	11485
Zircon_43_058	2135	0.24	7.11	0.20	2.32	3.95	0.83	28.67	13.02	176.70	68.92	318.83	693.05	132.20	12884
Zircon_44_059	3553	0.03	3.39	0.11	2.11	5.85	0.25	51.82	21.73	297.75	113.57	525.00	1130.66	216.00	17264
Zircon_45_060	876	0.13	3.55	0.12	0.90	1.68	0.32	11.42	5.25	68.47	27.73	132.31	311.04	60.75	11348
Zircon_46_062	3958	0.02	3.78	0.09	2.83	7.30	0.20	58.66	25.64	338.20	131.83	596.89	1291.98	242.80	20265
Zircon_47_063	2512	0.03	2.22	0.07	1.59	4.66	0.16	36.03	15.58	212.04	81.32	378.79	792.54	148.74	13457
Zircon_49_065	2466	0.11	3.32	0.17	2.06	5.34	0.78	37.11	15.89	209.01	79.83	362.50	784.27	147.52	13604
Zircon_50_066	2288	0.22	2.63	0.11	1.52	4.68	0.25	33.48	14.37	194.24	73.11	340.21	729.22	138.30	12166

Table 3. Coordinates of pegmatite locations.

Pegmatite body name	Location	
	Latitude	Longitude
La Ofelia	16°46'14"N	96°51'58"W
La Panchita	16°38'56"N	96°51'35"W
AYQ25-7	16°38'35"N	96°51'18"W
176-1	16°36'46"N	96°42'49"W
183-2	16°42'03"N	96°52'50"W
213-1	16°43'37"N	96°53'05"W
OC22-4AB	16°31'17"N	96°44'13"W

988 to 1267 Ma, with a mean age of 1201.2 ± 4.8 Ma (MSWD = 1.4), whereas zircon rims yielded 6 U-Pb ages, ranging from 965 to 1069 Ma. These 6 ages are dispersed and two of them are slightly discordant. The mean age for this younger age group was not calculated (Figure 2r). The Hf content of the analyzed zircons varies ranging from 7090 to 20265 ppm (avg = 13182), whereas Y ranges between 514 and 3958 ppm (avg = 1931). Th/U has variable ratios (0.07 – 0.23) and do not show much dependence from age. The REE patterns steeply increase from La to Lu (Lu_N/La_N avg = 7703) and are somewhat variable on the LREE side, with some spots showing relative LREE enrichments (Figure 2s). The Nd concentrations vary from 0.55 to 5.9 ppm. Grains with LREE enrichment have weaker Ce (e.g., $Ce/Ce^* = 2$) and Eu anomalies (e.g., $Eu/Eu^* = 0.28$). The LREE-depleted zircons have stronger Ce (e.g., $Ce/Ce^* = 7.9$) and Eu anomalies (e.g., $Eu/Eu^* = 0.04$).

DISCUSSION

Geochemistry

In general, the chondrite-normalized patterns of all zircon samples can be characterized by a steeply-rising slope from LREE to HREE, which can be defined by Lu_N/La_N values ranging from 1504 to 7703, and a different intensity of positive Ce and negative Eu-anomalies typical for igneous zircons (Hoskin and Schaltegger, 2003). Compared to classic granitic magmatic zircons, samples from our work are characterized by a similar LREE behavior, but a relatively higher HREE depletion (Figure 3). It should be noted that, in general, magmatic zircons have a trend of increasing REE content from ultramafic through mafic to granitic rocks (Belousova *et al.*, 2002). The zircon patterns of the Oaxacan Complex show similarity with zircon patterns of Phalaborwa Complex carbonatites in South Africa (Hoskin and Ireland, 2000). There are two types of REE patterns in the studied zircons: those with normalized Lu values that do not exceed 10^3 (183-2, 213-1, AYQ25-7, 176-1, La Panchita) and those with Lu values up to 10^4 (OC22-4AB, La Ofelia). Samples 176-1, 183-2 and 213-1 show patterns which are similar to each other.

Using the Ce/Ce^* vs. Eu/Eu^* genetic diagram of Belousova *et al.* (2002), the intensity of Ce and Eu anomalies in chondrite-normalized patterns can be evaluated. Pegmatites 213-1, 183-2, AYQ25-7 and La Ofelia have the same Eu anomaly size (Figure 4b), and the weakest Eu anomaly (Eu/Eu^* avg = 0.45) of this series is from La Panchita. All of the above zircon samples have very similar Ce anomalies. Sample OC22-04AB shows variable magnitudes of Ce (Ce/Ce^* vary from 2.0 to 15) and Eu (Eu/Eu^* vary from 0.015 to 0.7) anomalies. However, it should be noted that OC22-04AB has some spots with the weakest Ce ($Ce/Ce^* = 2$) and the most significant Eu ($Eu/Eu^* = 0.04$) anomaly among other samples. There is no age dependence of rims

and cores in regard to the REE and other trace element concentrations in all analyzed zircon grains. Likewise, there is not any significant relation between the Th/U ratios and the rim-core age difference. Most of the analyzed zircon samples (182-2, 213-1, La Ofelia and AYQ25-7) have high Th/U values, between 0.24 and 0.88. Only one sample (OC22-4AB) shows a relatively low Th/U ratio (from 0.06 to 0.2), that can be caused by its possible metamorphic genesis (e.g., Hoskin and Schaltegger, 2003; Rubatto, 2002). The interpretation of Th/U values is still in dispute, because it is not exactly known which are the values of the Th/U ratios in zircon for magmatic and metamorphic rocks and the distribution coefficients between zircon and melt at diverse P and T (e.g., Harley *et al.*, 2007).

The most unusual REE zircon patterns from this group of samples are from La Panchita pegmatite: it has the most pronounced Ce anomaly (average of $Ce/Ce^* = 43.3$), a weak Eu anomaly (Eu/Eu^* avg = 0.4) (Figures 3 and 4), a very steep slope of REE patterns (Lu_N/La_N avg = 6556) compared with other samples and strong HREE enrichment trends ($Lu_N/Gd_N = 37.6$). Its Eu anomaly is very small, probably due to the absence of any type of feldspars (plagioclase) in the genesis of this pegmatite.

Genetic diagrams

Shnukov *et al.* (1997), Pupin (2000) and Belousova *et al.* (2002) elaborated some diagrams which display concentrations of Hf, Y, U, Ce and Eu in zircons, with the aim to estimate the composition of the melt where zircons were crystallized (Figure 4). These diagrams are based on the theory that zircon grows in the early crystallization stages of igneous rocks and may strongly affect the behavior of many trace elements during magma crystallization (e.g., Nagasawa, 1970; Watson, 1979; Hoskin *et al.*, 2000; Belousova *et al.*, 2002).

According to Shnukov *et al.* (1997) and using a Hf (wt%) vs. Y (ppm) diagram, at least three groups of pegmatites can be discriminated (Figure 4a). (1) The first group (183-2, 213-1, 176-1) lies within the fields I, II and VI of “kimberlites”, “ultramafic, mafic and intermediate rocks” and “alkaline rocks and alkaline metasomatites of alkaline complexes”. It shows a relatively large range of Y (160 – 990 ppm) and Hf (9000 – 14000 ppm) concentrations. (2) The second group (OC22-04AB; La Ofelia) plots in the fields II and III of “ultramafic, mafic and intermediate rocks”, and “quartz-bearing intermediate and felsic rocks”. It has relatively moderate to high Y (450 – 3960 ppm) and high Hf contents (10000 – 20000 ppm). (3) The third group (La Panchita; AYQ25-7) straddle fields VI and VII of “alkaline rocks and alkaline metasomatites of alkaline complexes” and “carbonatites”. It can be characterized by moderate to low Y (120 – 770 ppm) and low Hf concentrations (5120 – 10700 ppm).

On the Ce/Ce^* versus Eu/Eu^* graph of Belousova *et al.* (2002) (Figure 4b) most analyses lie in the area of syenitic rocks; the exception is sample OC22-4AB, which displays scattered points. The Y (ppm) versus U (ppm) diagram (Figure 4c) shows that most of the analyses plot within the area of mafic and carbonatitic rocks (La Ofelia, AYQ25-7, 183-2, 176-1 and 213-1). Sample OC22-4AB points lie in the area of granitic rocks and La Panchita lies outside of all fields because of its high U concentrations (avg = 231 ppm) and moderate Y concentrations (avg = 262 ppm). The zircons which are most depleted in these elements are from sample AYQ25-7 ($Y \leq 400$ ppm and $U_{avg} = 63$ ppm). These diagrams of Belousova *et al.* (2002) should be interpreted together with other genetic diagrams (e.g., diagrams of Shnukov *et al.* (1997), Pupin (2000), and comparative REE pattern diagrams), as suggested by Hoskin and Schaltegger (2003). On the other hand, the fields for zircon-bearing rock types of Belousova *et al.* (2002) overlap each other at different degrees in most plots. A comparison of several plots or together with the Hf vs. Y diagram of Shnukov *et al.*

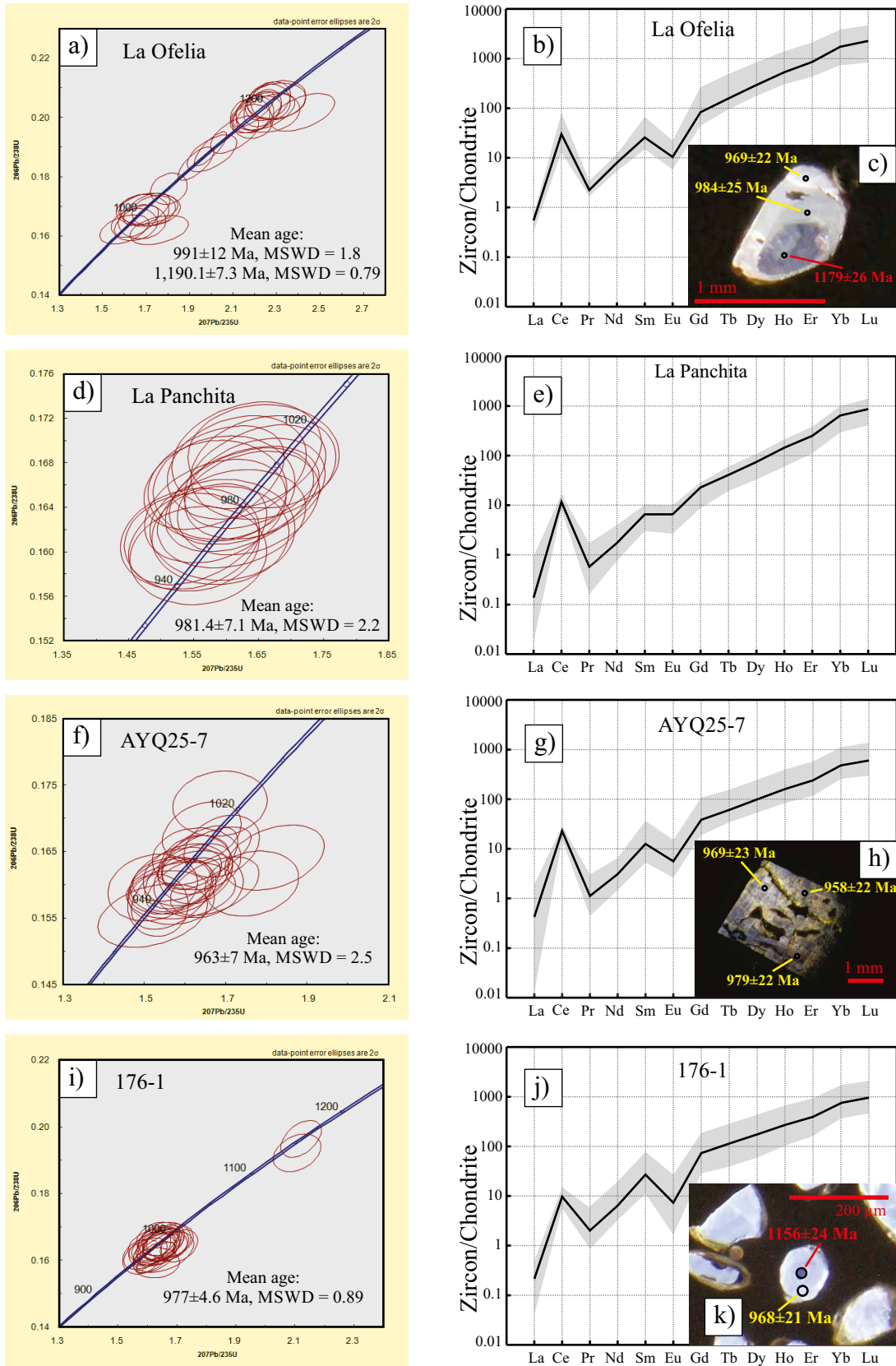


Figure 2. U-Pb concordia diagrams showing measured isotopic ratios with 2σ error ellipses and ages (a, d, f, i, o and r) and their chondrite-normalized (McDonough and Sun, 1995) REE plots for all analyzed spots (b, e, j, m, p and s). Black lines in REE plots represent the mean values. Representative cathodoluminescence (CL) images of analyzed zircon grains with marked laser ablation spots are also shown (c, h, k, n and t).

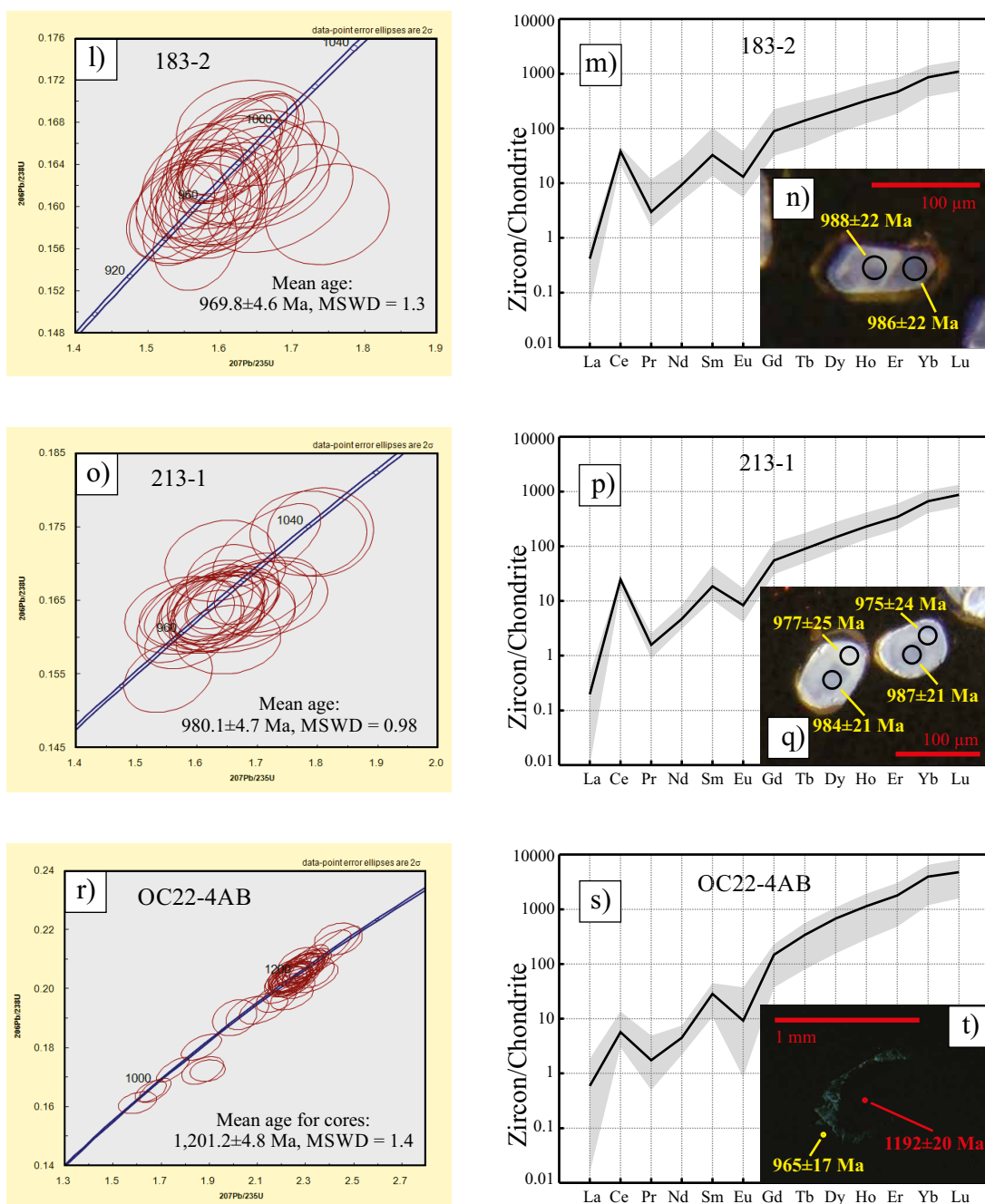


Figure 2 (cont.). U-Pb concordia diagrams showing measured isotopic ratios with 2σ error ellipses and ages (a, d, f, l, o and r) and their chondrite-normalized (McDonough and Sun, 1995) REE plots for all analyzed spots (b, e, j, m, p and s). Black lines in REE plots represent the mean values. Representative cathodoluminescence (CL) images of analyzed zircon grains with marked laser ablation spots are also shown (c, h, k, n and t).

with well-defined positive Ce/Ce^* (avg = 7.8) and negative Eu/Eu^* (avg = 0.23) anomalies (Figure 2p). The HREE enrichment is characterized by Lu_N/Gd_N avg = 15.5 and the average value of Sm_N/La_N is 91.7.

Pegmatite sample OC22-4AB

This pegmatite group is located 5 km to the south of Ejutla, along the road Ejutla-Miahuatlán. This is a group of 2 – 8 m wide and 12 – 35 m long pegmatite lenses, which follow the foliation of the biotite-garnet gneissic host rock. These pegmatite lenses are represented by a thin (some cm long) biotite-andesine border zone

and a central zone composed of deformed quartz, sericitized andesine, pyroxene (spodumene?), muscovite, primary calcite, abundant zircon and titanite central zone. Zircon crystals extracted from the central zone are euhedral, up to 500 μ m in length, and range in shape from moderately elongated to prismatic, with bipyramidal endings to ovoid or sub-spherical (“soccerball”) forms with well-defined faces, colored dark-red to purple. The zircon grains from this sample are almost non-luminescent, and their internal structure is hard to see, but we found some zircon crystals with dark cores and slightly light rims (Figure 2t). U-Pb ages obtained from 39 zircon cores range from

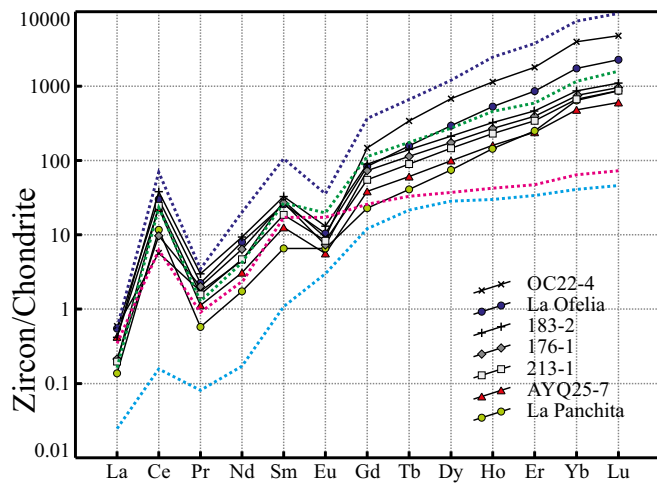


Figure 3. Mean chondrite-normalized REE compositions of zircon samples (black thin lines and symbols). Some bibliographical data is plotted for comparison: blue dotted line – granodiorite, Bogy Plain massif, Australia (Hoskin *et al.*, 2000); green dotted line – carbonatites, Phalaborwa complex, South Africa (Hoskin and Ireland, 2000); light blue dotted line – high-pressure metasediments, Sesia Zone, Southern Alps (Rubatto, 2002); pink dotted line – ultra-high-pressure gneisses, Kokchetav Massif, Kazakhstan (Hermann *et al.*, 2001).

(1997) and Y_2O_3 vs. HfO_2 graph of Pupin (2000) can help to identify zircons from different rock types.

Pupin (2000) elaborated the Y_2O_3 (ppm) versus HfO_2 (ppm) diagram basically for granitic rocks, but some special areas for basic to intermediate rocks are also included (Figure 4d). The group of samples 183-2, 213-1 and 176-1 lies in the field of “basic to intermediate calc-alkaline rocks” and the La Panchita sample is positioned in the “peralkaline syenites” field. It is difficult to make a petrogenetic conclusion, based only on these diagrams, but at least it is shown that the geochemical nature of some of the studied pegmatites must have been related to the presence of ultramafic-alkaline precursors, probably unrelated to granitic *sensu lato* magmas.

Geochronology

There are three types of pegmatites according to their crystallization ages (Figure 5). The first group is represented by samples AYQ25-7, 183-2 and 176-1. Their mean ages are in the range of 963 ± 7 to 977 ± 4.6 Ma. This age range can be described as post-tectonic (Anderson and Silver, 1971), with respect to the last episode of the Grenville orogeny (Zapotecan orogeny: 1004 to 978 ± 3 Ma) in the Oaxacan Complex (Solari *et al.*, 2003) (Figure 5). Sample 176-1 has also two older ages of 1156 ± 24 and 1134 ± 25 Ma, which are interpreted as xenocrystic cores.

The second group is represented by samples taken from pegmatite bodies of La Panchita and 213-1. The mean ages of these samples are almost identical, 981.4 ± 7.1 and 980.1 ± 4.7 Ma (Figure 5), respectively. La Panchita pegmatite did not suffer any type of metamorphism but, as it was mentioned before, the 213-1 pegmatite lenses show migmatitic features (Mehnert, 1968), so they must have been formed during a high grade metamorphic event. La Panchita and 213-1 pegmatite bodies were formed during the same time period, corresponding to the last stage of the Zapotecan orogeny (Solari *et al.*, 2003). The distance between La Panchita and 213-1 is ~ 10 km and it is noteworthy that they have different metamorphic grades. One of the several possibilities is that the uncertainty of the LA-ICP-MS U-Pb method is underestimated. If we look at the age dispersion for La Panchita and ignore the

statistical calculations, we can conclude that its age is post-tectonic. This is coherent with the rest of the available data and suggests an age of 978 – 980 Ma for the last episode of granulite facies metamorphism. More data are necessary to resolve this issue.

The third group is represented by pre-tectonic pegmatite bodies such, as La Ofelia and OC22-4AB. Zircon cores of OC22-4AB have a mean crystallization age of 1201.2 ± 4.8 Ma (Figure 5) and dispersed ages of recrystallized rims in the range of 965 ± 17 to 1069 ± 20 Ma. The dispersion and discordance of these ages could be the result of Pb-loss during the granulite facies metamorphism. Metamorphic overprints are also indicated by some distinctive features, like the deformation of the pegmatite body, the “soccerball” zircon morphology and relative low Th/U ratios. Zircons from La Ofelia pegmatite also show these two age groups. The oldest ages are represented by cores with a mean age of 1190.1 ± 7.3 Ma and the younger ages are represented by rims with a mean age of 991 ± 12 Ma. There are also some spots with intermediate concordant ages (1045 ± 23 ; 1091 ± 25 ; 1114 ± 28 and 1119 ± 25 Ma) which we interpret as mixed ages, probably a result of analyzing the limit between cores and rims. There is a clear relation between metamorphic rims, older cores and the irregular zircon morphology.

General discussion

The U-Pb LA-ICP-MS ages obtained from zircons confirmed the pre-tectonic (“old”), syn-tectonic and post-tectonic division of all pegmatites (Solari *et al.*, 1998) (Figure 5). The ages of post-tectonic pegmatites obtained in this work vary from 963 ± 7 to 977 ± 5 Ma. The syn-tectonic pegmatites, formed during the last phase of the Oaxacan Complex Orogeny (Zapotecan) have an age of 981 ± 7 Ma. The “old” pegmatites formed during the period between 1190 ± 7 and 1201 ± 5 Ma. These “old” pegmatite bodies do not show any ages that can be interpreted as being part of the Olmecan orogeny (1106 ± 6 Ma). The youngest ages of OC22-4AB define a range of ages between 965 ± 17 and 1069 ± 20 Ma, which is the result of different degrees of Pb loss in zircons during the Zapotecan orogeny (from 1004 to 978 ± 3 Ma, Solari *et al.*, 2003).

The zircon geochemistry shows that all studied pegmatite intrusions, with the exception of OC22-4AB, are not “granitic” pegmatites at all, which is in contrast with previous works (Haghenbeck-Correa, 1993; Arenas-Hernández, 1999). This means that pegmatites from the central portion of the Oaxacan Complex reflect the composition of non-granitic rocks or melts. The zircon trace element geochemistry shows that La Panchita pegmatite has been formed during the evolution of an alkaline and SiO_2 -depleted melt, like carbonatite or syenitic rocks. The group of pegmatites 183-2, 176-1, 213-1 and La Ofelia shows similar chemical behavior and a possible mafic composition of the source rock type. AYQ25-7 has transitional trace element patterns between La Panchita pegmatite and the group of 183-2, 176-1 and 213-1. Only one zircon sample, that from OC22-4AB, shows a granitic type initial composition of this pegmatite body.

With respect to pegmatite generation, it should be noted that the pegmatites studied in this work could have three different ways of formation: pure magmatic, pure metamorphic, and a mixture of magmatic and metamorphic processes. The first is the classical process of formation during the last stage of magmatic intrusions (London and Černý, 2008). The second way implies a pegmatite formation by partial melting or anatexis of the Oaxacan Complex rocks during high-grade metamorphism, without involving magma melt from another source (Mehnert, 1968). All previous authors (Haghenbeck-Correa, 1993; Schaaf and Schulze-Schreiber, 1998; Arenas-Hernández, 1999) claim the anatexis way for the Oaxacan Complex pegmatite formation. The third and last possible mode of

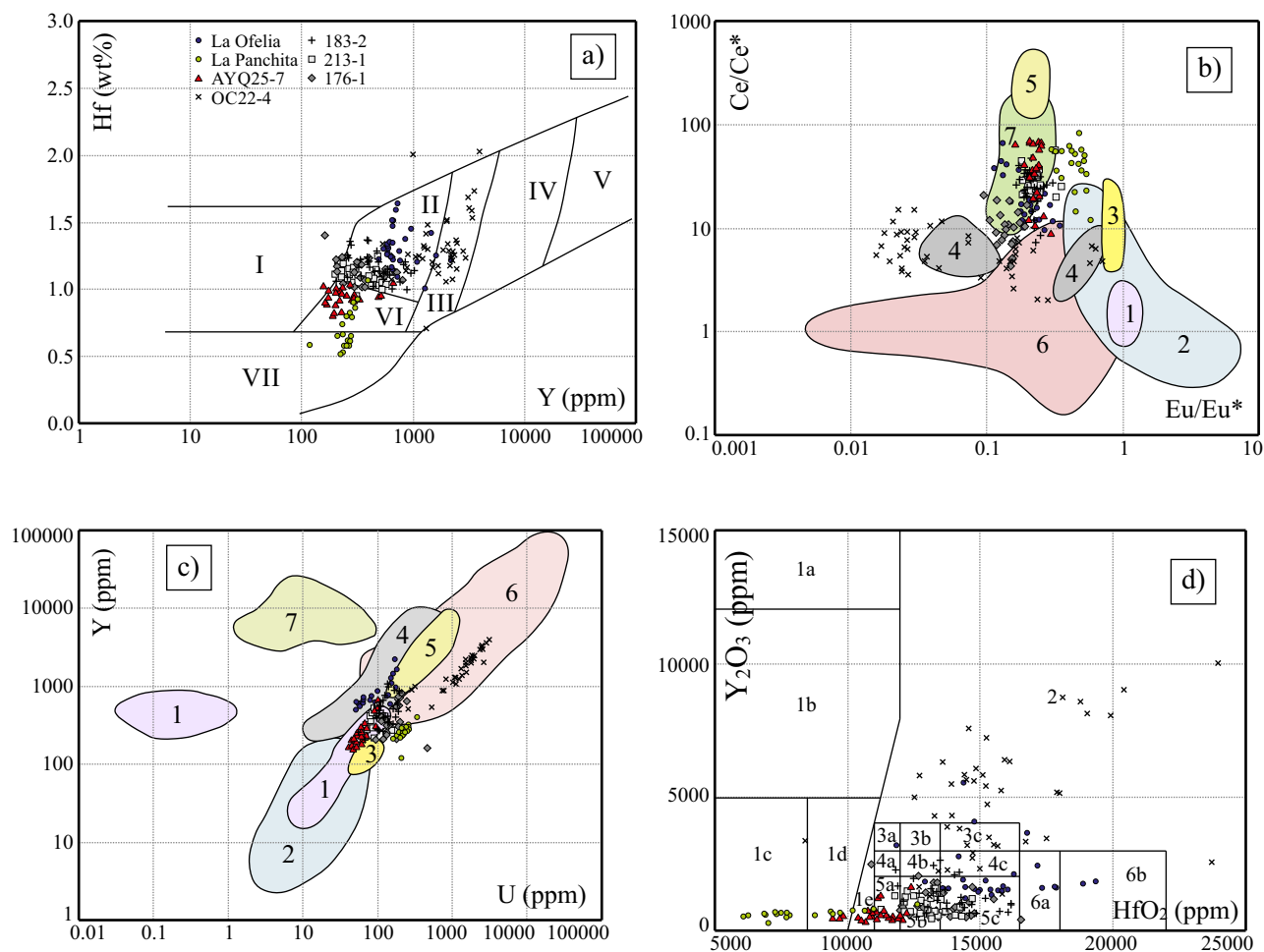


Figure 4. a) Plot of Hf vs. Y concentration in zircons (Shnukov *et al.*, 1997). Legend: I – kimberlites; II – ultramafic, mafic and intermediate rocks; III – quartz-bearing intermediate and felsic rocks; IV – felsic rocks with high SiO₂ content; V – greisens; VI – alkaline rocks and alkaline metasomatites of alkaline complexes; VII – carbonatites. b) Ce/Ce* vs. Eu/Eu* diagram and c) Y vs. U distribution behavior in zircons according to the origin of their protolith (Belousova *et al.*, 2002). Legend: 1- carbonatites; 2 – kimberlites; 3 – syenites; 4 – mafic rocks; 5 – syenite pegmatites; 6 – granitoids; 7 – nepheline syenites and syenite pegmatites. d) Plot of Y₂O₃ vs. HfO₂ showing petrological environments for zircon crystallization, after Pupin (2000). Legend: 1a – tholeiitic plagiogranites; 1b-c-d-e – hypersolvus alkaline granites; 1c-d-e – peralkaline syenites; 1c – alkali basalts; 1e, 2, 3a-b-c, 4a-b-c – subsolvus alkaline granites; 4a-b-c, 5a-b-c, 6a-b – basic to intermediate calc-alkaline rocks; 5a-b-c – calc-alkaline granites; 4a-b, 5a-b-c – high-K calc-alkaline, or Mg-K granites; 4c, 5a-b-c – subalkaline or Fe-K granites; 3b-c; 4b-c, 5b-c, 6a-b – peraluminous porphyric granites; 3c, 4c, 5c, 6a – peraluminous leucogranites.

pegmatite formation is a mixture of the two aforementioned processes: partial melting of the Oaxacan Complex rocks during high grade metamorphism involving foreign magma melt from another source (Mehnert, 1968).

It seems that the studied zircons have magmatic REE compositions rather than metamorphic (Figure 3), which means that they underwent a magmatic mechanism of formation; but according to Hoskin and Schaltegger (2003), the composition of metamorphic zircon in equilibrium with an anatectic melt does not differ greatly from igneous zircon. So it is difficult to give a final opinion about the magmatic, metamorphic or hybrid process of pegmatite formation using only trace element chemistry of zircons.

The relation between a magmatic source, as derived from zircon geochemistry and the U-Pb data, suggests that post-tectonic pegmatites originated from an anorogenic magmatic source are related to a post-Grenvillian rifting event; syntectonic pegmatites are probably derived from a hybrid magma, and the origin of “old” pegmatites still cannot be discerned with the current available data.

CONCLUSIONS

From the geochemical and geochronological study of zircons from seven pegmatites located in the Oaxacan Complex, Oaxaca, México, we can conclude the following:

- The numerous pegmatites in this complex can be roughly divided into granitic, displaying a simple quartzo-feldspathic mineralogy and non-granitic, showing a less-common mineralogy with pyroxenes, scapolite, large zircon or calcite.
- The obtained ages confirm the division in pre-tectonic (~1200 Ma), syntectonic (~980 Ma) and post-tectonic (<980 Ma) time of the pegmatite formation.
- The Olmecan orogeny cannot be identified in the central part of the Oaxacan Complex with the available data.
- The selected pegmatites for this study, mainly non-granitic in nature, indicate the presence of mafic and alkaline parental magmas for these intrusives.
- The application of geochemical discrimination diagrams for

- Geosystems, 11(3), doi:10.1029/2009GC002618.
- Petrus, J.A., Kamber, B.S., 2012, VizualAge: A novel approach to laser ablation ICP-MS U-Pb geochronology data reduction: *Geostandards and Geoanalytical Research*, 36(3), 247–270.
- Prol-Ledesma, R.M., Melgarejo, J.C., Martín, R. F., 2012, The el Muerto “NYF” granitic pegmatite, Oaxaca, Mexico, and its striking enrichment in allanite-(Ce) and monazite-(Ce): *The Canadian Mineralogist*, 50(4), 1055–1076.
- Pupin, J.P., 1980, Zircon and granite petrology: *Contributions to Mineralogy and Petrology*, 73(3), 207–220.
- Pupin, J.P. 2000, Granite genesis related to geodynamics from Hf-Y in zircon: *Transactions-Royal Society of Edinburgh*, 91(1/2), 245–256.
- Rubatto D, 2002, Zircon trace element geochemistry: partitioning with garnet and the link between U-Pb ages and metamorphism: *Chemical Geology*, 184, 123–138.
- Ruiz, J., Tosdal, R.M., Restrepo, P.A., Murillo-Muñetón, G., 1999, Pb isotope evidence for Colombia-southern Mexico connections in the Proterozoic: *Geological Society of America, Special Paper*, 336, 183–198.
- Schaaf, P., Schulze-Schreiber, C.H., 1998, Pegmatites in the Oaxacan Complex, Southern Mexico, Isotopic dating and genetical aspects: Published as a supplement to *Eos, Transactions, AGU*, 79(45).
- Schulze-Schreiber, C.H., 2011, *Petrología y geoquímica de las rocas de Pluma Hidalgo, Oaxaca e implicaciones tectónicas para el Proterozoico de “Oaxaquia”*: Instituto de Geología, Postgrado en Ciencias de la Tierra, Universidad Nacional Autónoma de México, Tesis Doctoral, 341 pp.
- Schulze-Schreiber, C., Keppie, J.D., Ortega Rivera, A., Ortega-Gutiérrez, F., Lee, J.W.K., 2004, Mid-Tertiary cooling ages in the Precambrian Oaxacan Complex of Southern Mexico: indication of exhumation and inland arc migration: *Revista Mexicana de Ciencias Geológicas*, 21(2), 203–211.
- Shnukov, S.E., Andreev, A.V., Savenok, S.P., 1997, Admixture elements in zircons and apatites: a tool for provenance studies of terrigenous sedimentary rocks *en* EUG IX conference 23–27 March 1997: Strasbourg, France, European Union of Geosciences, Abstract 65/4P16:597.
- Solari, L.A., Lopez, R., Cameron, L.K., Ortega-Gutiérrez, F., Keppie, J.D., 1998, Reconnaissance U/Pb geochronology and common Pb isotopes from the northern portion of the 1 Ga Oaxacan Complex, Southern Mexico: Published as a supplement to *Eos, Transactions, AGU*, 79(45).
- Solari, L.A., Keppie, J.D., Ortega-Gutiérrez, F., Cameron, K.L., Lopez, R., Hames, W.E., 2003, 990 Ma and 1, 100 Ma Grenvillian tectonothermal events in the northern Oaxacan complex, southern Mexico: roots of an orogeny: *Tectonophysics*, 365, 257–282.
- Solari, L.A., Gómez-Tuena, A., Bernal, J.P., Pérez-Arvizu, O., Tanner, M., 2010, U-Pb zircon geochronology by an integrated LA-ICP-MS microanalytical workstation: Achievements in Precision and Accuracy: *Geostandards and Geoanalytical Research*, 34(1), 5–18.
- Watson, E.B., 1979, Zircon saturation in felsic liquids: experimental results and applications to trace element geochemistry: *Contributions to Mineralogy and Petrology*, 70(4), 407–419.
- Weber, B., Scherer, E.E., Schulze, C., Valencia, V.A., Montecinos, P., Mezger, K., Ruiz, J. 2010, U–Pb and Lu–Hf isotope systematics of lower crust from central-southern Mexico—Geodynamic significance of Oaxaquia in a Rodinia Realm: *Precambrian Research*, 182(1), 149–162.

Manuscript received: November 20, 2013

Corrected manuscript received: January 23, 2015

Manuscript accepted: February 1, 2015